DALE ANDERSON
JERALD VOGEL

JULY 1971

FINAL REPORT
ISU-ERI-AMES-71015

NUMERICAL SOLUTION OF FLOWFIELDS BEHIND RECTANGULAR WINGS

NASA Grant No. NGR 16-002-029

Project 859-S

ENGINEERING RESEARCH

ENGINEERING RESEARCH

ENGINEERING RESEARCH

ENGINEERING RESEARCH

ENGINEERING RESEARCH

FINAL REPORT

NUMERICAL SOLUTION OF FLOWFIELDS BEHIND RECTANGULAR WINGS

Dale Anderson
Jerald Vogel

July 1971

Grant No. NGR 16-002-029
ISU - ERI - AMES - 71015
Project 859-S

ENGINEERING RESEARCH INSTITUTE
IOWA STATE UNIVERSITY AMES

CONTENTS

NUMERICAL SOLUTION OF FLOW FIELDS BEHIND RECTANGULAR WINGS

Dale Anderson and Jerald Vogel

ABSTRACT

This paper summarizes research accomplished under NASA Grant NGR 16-002-029 for the period 1 July 1970 through 30 June 1971. Research accomplished during this period includes: (1) evaluation of various differencing methods applied to the hyperbolic partial differential equations encountered in gas dynamics; (2) application of the apparent best numerical differencing techniques to the modified Burger's equation, wedge flow, two-dimensional shock reflection and the three-dimensional finite thickness wing at zero angle of attack; and (3) calculation of preliminary results for wedge flows using optimum differencing methods. Recommendations for continued research are presented and include completion of the rectangular wing problem at angle of attack, initiation of work on delta wing configurations and continued exploration of near-optimum computing techniques.

NUMERICAL SOLUTION OF FLOW FIELDS BEHIND RECTANGULAR WINGS

INTRODUCTION

Aerodynamic analysis of aircraft capable of operating at supersonic speeds for extended periods of time is a formidable task. The complex geometry of such aircraft and the difficulty of solving the equations governing the aerodynamics preclude the possibility of obtaining exact solutions for the flow field. These fundamental difficulties have prompted the development of numerous approximate methods for analyzing fluid flow. One of the most common of the simplifying assumptions used is that the flow may be separated into a viscous boundary layer flow and an outer inviscid flow which effectively determines the body pressure. This report is concerned with the calculation of the outer inviscid flow about a rectangular wing moving at supersonic speeds.

The inviscid equations of motion governing the flow generated by a wing moving at supersonic speeds form a set of hyperbolic partial differential equations. Since they are hyperbolic, the equations can be solved (at least conceptually) by techniques applicable to initial value problems. At present only two such techniques which provide exact solutions have been applied to inviscid supersonic flow problems. The first technique is the method of characteristics. This method has been successfully applied to numerous supersonic flow problems. Unfortunately, the application of this method is a complex task due to the geometric problems introduced by body shape, the coordinate system or systems required and the inherent way in which a characteristics method works. The second method is to use finite difference approximations of the equations of motion and solve the resulting approximate equations

at each grid or mesh point. This provides a solution for the inviscid flow throughout the flowfields.

Numerical calculations of inviscid flows based upon the full Eulerian equations have been carried out for a variety of supersonic problems using several numerical techniques. These numerical techniques have been developed to the point where they can be relied upon to give acceptable results for flow about aerodynamic shapes moving at supersonic speeds generating shocks of nonuniform intensity which surround the disturbed region of fluid. The methods are usually first, second or third order. Numerous authors have applied the Lax first-order method to fluid flow problems. Notable among these are the time dependent blunt body solutions obtained by Bohachevsky and Rubin[1] and Bohachevsky and Mates[2] and the nonequilibrium gas dynamic calculations of DeJarnette.[3] While the Lax method provides reasonable results for very small mesh sizes, second-order methods are being used with increasing frequency. Kutler[4] has recently applied a version of the second-order Lax-Wendroff method developed by MacCormack[5] to flow about sonic-edged, conical, wing-body combinations at angle of attack. Results of his work show excellent agreement with conical flow solutions calculated using other methods and with available experimental data.

The present paper is concerned with application of the second-order MacCormack[5] method and the more recently developed third-order Rusanov[6] method to the solution of the full Eulerian equations for flow about a rectangular wing moving supersonically. The results of a number of simple nonlinear problems are presented. Solutions of the simple Burger's equation, wedge flow and shock reflection were calculated to

aid in understanding the MacCormack and Rusanov differencing methods and their application to hyperbolic systems. The flow field generated by a rectangular wing at zero angle of attack was calculated and results are presented for a free stream Mach No. of 2. These are the only results available on the three-dimensional wing problem at this time. The results for the zero angle of attack case appear to be satisfactory with application of proper boundary conditions occurring as the only major difficulty. The angle of attack case is currently in the program de-bug stage and results will be published as they become available. In addition a brief summary of preliminary work on development of optimum differencing methods is presented.

DIFFERENCING METHODS

Differencing methods representative of first-order, second-order and newer third-order techniques are presented in this section. The application of each of these methods to the nonlinear equation

$$\frac{\partial E}{\partial t} + \frac{\partial F}{\partial x} = 0 \tag{1}$$

is discussed. The stability requirement for each of the methods is presented and derivation of the modified equation associated with the wave equation for each method is presented.

Lax's Method

Lax derived a first-order difference method which he used in calculating one-dimensional flow containing shock waves.[7] Time derivatives were approximated by

$$\frac{\partial E}{\partial t} = \frac{E_j^{n+1} - \frac{E_{j+1}^n + E_{j-1}^n}{2}}{\Delta T} \tag{2}$$

while space derivatives were approximated by

$$\frac{\partial F}{\partial x} = \frac{F_{j+1}^n - F_{j-1}^n}{2\Delta x} \tag{3}$$

Applying this to Eq. (1) yields the following at the (n + 1) time point

$$E_j^{n+1} = \frac{E_{j+1}^n + E_{j-1}^n}{2} - \frac{\Delta T}{2\Delta x}\left[F_{j+1}^n - F_{j-1}^n\right] \tag{4}$$

This technique is required to satisfy the usual stability requirement, i.e.

$$\left|\sigma_{max} \frac{\Delta T}{\Delta x}\right| \leq 1 \tag{5}$$

where σ_{max} is the maximum eigenvalue of the Jacobian $\partial F/\partial E$.

Lax's method is particularly easy to use because storage and computation time requirements are small. In addition, all calculations are done on the same level, i.e., data at time t are used to directly obtain values at time $t + \Delta t$ in one step. Unfortunately, Lax's method possesses an implicit artificial viscosity which causes considerable shock smearing when the method is used at off-design Courant numbers.

If the Lax method is applied to the one-dimensional wave equation

$$\frac{\partial u}{\partial t} + c \frac{\partial u}{\partial x} = 0 \tag{6}$$

The resulting difference expression becomes

$$u_j^{n+1} = \frac{1}{2} (u_{j+1}^n + u_{j-1}^n) - c \frac{\Delta T}{\Delta x} \left(\frac{u_{j+1}^n - u_{j-1}^n}{2} \right) \tag{7}$$

If a Tayor series expansion is written for each of the terms in this expression, the following so-called modified equation is obtained

$$\frac{\partial u}{\partial t} + c \frac{\partial u}{\partial t} = \frac{\Delta x^2}{2\Delta T} [1 - \nu^2] u_{xx} - c \frac{\Delta x^2}{6} [1 - \nu^2] u_{xxx} + \ldots \tag{8}$$

This equation is really the one the difference method solves. The first nonzero term on the right-hand side represents the order of the differencing method and a remainder which goes to zero only at a Courant number of one, i.e., the design point. This means the solution is truly a solution of the wave equation only when $\nu = c\ \Delta T/\Delta x = 1$. If $\nu \neq 1$, the solution satisfies the modified Eq. (8). This will be discussed in detail in later sections.

Lax's method has been used by numerous authors in solving complex fluid flow problems.[1-3]

MacCormack's Method

MacCormack has constructed a second-order preferential, predictor-corrector sequence for use in solving systems of equations in conservative form.[9] When applied to Eq. (1), MacCormack's method reads:

$$\tilde{E}_j^{n+1} = E_j^n - \frac{\Delta T}{\Delta x}[F_{j+1}^n - F_j^n]$$

$$E_j^{n+1} = \frac{1}{2}\left[E_j^n + \tilde{E}_j^{n+1} - \frac{\Delta T}{\Delta x}[\tilde{F}_j^{n+1} - \tilde{F}_{j-1}^{n+1})\right] \tag{9}$$

This method contains a forward difference in the predictor and a backward difference in the corrector. MacCormack[5] and Kutler[4] have used this technique on shocked flows and have obtained good results.

MacCormack's method satisfies the same stability requirement as Lax's, namely

$$\left|\sigma_{max} \frac{\Delta T}{\Delta x}\right| \leq 1$$

More storage and computing time are required than with Lax's method. However, much better flow field resolution is obtained for the same size mesh. The main reason is the higher order of the method and the elimination of the implicit artificial viscosity.

MacCormack's method applied to wave Eq. (6) becomes

$$\tilde{u}_j = u_j^n - c\,\frac{\Delta T}{\Delta x}[u_{j+1}^n - u_j^n]$$

$$u_j^{n+1} = \frac{1}{2}\left[u_j^n + \tilde{u}_j^{n+1} - c\,\frac{\Delta T}{\Delta x}(\tilde{u}_j^{n+1} - \tilde{u}_{j-1}^{n+1})\right] \tag{10}$$

If the predictor is substituted into the corrector, the following modified differential equation is formed

$$\frac{\partial u}{\partial t} + c\frac{\partial u}{\partial x} = -c\frac{\Delta x^2}{6}(1-\nu^2)u_{xxx} - c\frac{\Delta x^3}{8}\nu(1-\nu^2)u_{xxx} + \ldots \tag{11}$$

The same information is clearly obtained here as in the case of the Lax method, i.e., MacCormack's method is second order and provides a solution to the wave equation under the condition that $\nu = 1.0$. It is important to note that the first nonzero term on the right-hand side of the modified equation is second order, and as a result produces a more nearly exact solution than Lax's method for any Courant number.

Rusanov's Method

With the advent of large high-speed computers, higher-order differencing methods are being applied to fluid mechanics problems. One of the most recent is a third-order method developed simultaneously by Rusanov[6] and Burstein and Mirin.[8] This technique uses a three-level predictor-corrector sequence, and when applied to Eq. (1) becomes

$$\begin{aligned}
E^{(1)}_{j+1/2} &= \frac{1}{2}(E^n_{j+1} + E^n_j) - \frac{\Delta T}{3\Delta x}(F^n_{j+1} - F^n_j) \\
E^{(2)}_j &= E^n_j - \frac{2\Delta T}{3\Delta x}(F^{(1)}_{j+1/2} - F^{(1)}_{j-1/2}) \\
E^{n+1}_j &= E^n_j - \frac{\Delta T}{24\Delta x}[-2F^n_{j+2} + 7(F^n_{j+1} - F^n_{j-1}) + 2F^n_{j-2}] \\
&\quad - \frac{3\Delta T}{8\Delta x}(F^{(2)}_{j+1} - F^{(2)}_{j-1}) \\
&\quad \frac{\delta}{24}[E_{j+2} - 4(E_{j+1} + E_{j-1}) + 6E_j + E_{j-2}]
\end{aligned} \tag{12}$$

The derived term in the third level is required for stability of the system. The stability bounds or requirements are

$$\left|\sigma_{max} \frac{\Delta T}{\Delta x}\right| \leq 1, \text{ i.e., } \nu \leq 1$$

and (13)

$$4\nu^2 - \nu^4 \leq \delta \leq 3$$

This method also requires more computing time and storage, however, the increase in accuracy may justify its use.

If Rusanov's method is applied to the wave equation, the modified equation produced is

$$\frac{\partial u}{\partial t} + c \frac{\partial u}{\partial t} = - c \frac{\Delta x^3}{24} \left(\frac{3\delta}{\nu} - 4\nu + \nu^3\right) u_{xxxx}$$

$$- c \frac{\Delta x^4}{120} (15\delta - 4 - 15\nu^2 + 4\nu^4) u_{xxxxx} + \ldots \quad (14)$$

As a result of the δ parameter, the modified equation has a double requirement if an exact solution of the wave equation is to be formed. The requirement is that $\nu = 1.0$ and that $\delta = 3.0$. This, of course, represents the stability limit as in the previous methods and can be interpreted as a single requirement since the δ parameter must take on the value of 3 as ν approaches 1 for a stable system. In addition, the first nonzero term on the right-hand side is third order, consistent with the differencing method.

SOLUTION OF THE MODIFIED BURGER'S EQUATION

One of the major problems encountered in applying finite difference methods to fluid flow problems is the variation of the eigenvalue structure of the equations of motion in the flow field. This is important because the eigenvalue structure determines the stability bound for the difference method and also the so-called design point of operation, e.g., a Courant number of one. An investigation of the behavior of two numerical methods is presented here with particular emphasis on the spreading of discontinuities and oscillations of the solution near points of rapid change of the dependent variable.

The hyperbolic form of the equation introduced by J. M. Burger is a valuable aid for use in studying the ability of a given numerical method to produce a solution to a nonlinear equation.[9] The modified Burger's equation in conservative form reads

$$\frac{\partial u}{\partial t} + \frac{\partial}{\partial x}\left(\frac{u^2}{2}\right) = 0 \tag{15}$$

Kutler has successfully used this equation as an analog of the inviscid Euler equations and studied the solutions produced using various numerical algorithms.[4] In particular, Kutler examined first- and second-order methods normally used in solving the gas dynamic equations.

Kutler's results indicate that MacCormack's method provided the most satisfactory results from among those he examined. Since his investigation, third-order schemes such as that developed simultaneously by Rusanov[6] and Burstein and Mirin[8] have started to appear. The Rusanov technique has been developed specifically for application to hyperbolic systems written in conservative form. The results presented

here compare only MacCormack's method with the Rusanov technique. This provides a comparison of what in Kutler's opinion is one of the best second-order methods available with a more recently developed third-order technique.

The problem is to determine the solution of the modified Burger's equation subject to initial conditions shown in Fig. 1, which are

$$u = 0 \qquad x \geq x_1$$

$$u = u_1 \qquad x_1 > x > x_2$$

$$u = u_2 \qquad x \leq x_2$$

where $u_2 > u_1$.

Since this problem represents the intersection of two discontinuities, the exact solution must be represented in two regions: the first region is prior to the intersection of the discontinuities and the second is after the intersection (Fig. 2). The exact solution in these regions is

Region 1

$$u(x, t) = 0 \qquad \frac{x - x_1}{t} > \frac{u_1}{2}$$

$$u(x, t) = u_1 \qquad x_2 + \frac{u_1 + u_2}{2} t \leq x \leq x_1 + \frac{u_1 t}{2}$$

$$u(x, t) = u_2 \qquad \frac{x - x_2}{t} < \frac{u_1 + u_2}{2}$$

Region 2

$$u(x, t) = 0 \qquad \frac{x}{t} > \frac{u_2}{2}$$

$$u(x, t) = u_2 \qquad \frac{x}{t} \leq \frac{u_2}{2}$$

The first double shock considered was provided with $u_1 = 3$ and $u_2 = 5$. The mesh used was 100 points long in the x-direction with $x_1 = 15$ while $x_2 = 36$. The discontinuities appearing in the initial data are assumed to be spread over one mesh interval. The results of applying Rusanov's and MacCormack's methods to this problem are shown in Figs. 3 and 4. The Courant number is unity in both cases while the δ parameter in the Rusanov method is chosen to be 3 as required by the linear stability bound. The wave position and amplitude appear to be correctly predicted by both methods. It is very important to notice that the Rusanov method produces more oscillations than does MacCormack's. In addition, it should be noted that the u = 3 amplitude wave initially is being computed at an effective Courant number of 0.6. This is off-design for both methods and produces some additional oscillations about the discontinuity and also causes the discontinuities to spread out over several mesh intervals. It is surprising that the second-order MacCormack method appears to produce much crisper shocks with fewer oscillations at off-design than the higher-order Rusanov method.

A 5-1-0 problem was solved providing a factor of five in Courant number variation in the field. The results are presented in Figs. 5 and 6 and indicate the same trends as the 5-3-0 problem, namely that the MacCormack method produces better shock resolution with fewer oscillations over the range of effective Courant numbers considered.

Some additional runs were made with the Rusanov method to determine the accuracy of the stability bound based on the linear analysis. It was determined that values of the Courant number considerably larger

than one could be used in solving problems. In addition, the lower stability bound on the δ parameter can be violated without producing unstable solutions. Figures 7-10 present results obtained by using the Rusanov method on both the 5-3-0 and 5-1-0 problem but at values of δ outside the linear stability bound. The results shown in Figs. 7 and 8 are satisfactory, and one may conclude that the method might be used at smaller than recommended δ values and still obtain useful results. However, the question of how small δ may be has yet to be resolved. Figures 9 and 10 present solutions to the same problem with $\delta = 1$. These results certainly are not as satisfactory as those previously obtained. The oscillations produced are quite pronounced, and for large time oscillations appear to have the character of a limit cycle. They seem to increase in amplitude for some time then stabilize to a relatively constant amplitude. It appears that a δ value of two produces the best results when the Courant number is unity.

On the basis of information obtained from the solutions of Burger's equation, use of the MacCormack method is to be preferred over Rusanov's technique. Shock resolution and over- and under-shoot characteristics are better over the range of eigenvalues considered. In addition, the computer storage and computation times required are significantly lower for the MacCormack method as compared to Rusanov's. Additional comparative analysis is presented in later sections.

TWO-DIMENSIONAL WEDGE STUDY

A study utilizing the two-dimensional wedge was undertaken to further develop the comparison between the second-order MacCormack technique and the third-order technique developed by Rusanov. In addition, various coordinate systems were briefly investigated to gain experience in the application of the two numerical techniques and to aid in the choice of a good coordinate system for the three-dimensional tip problem.

Using an approach similar to Kutler's, the wedge flow equations of motion in a Cartesian body oriented coordinate system for a steady, inviscid, nonheat-conducting and adiabatic flow are given by[4]

$$\begin{aligned}
&\frac{\partial}{\partial x}(\rho u) + \frac{\partial}{\partial y}(\rho v) = 0 \\
&\frac{\partial}{\partial x}(p + \rho u^2) + \frac{\partial}{\partial y}(\rho uv) = 0 \\
&\frac{\partial}{\partial x}(\rho uv) + \frac{\partial}{\partial y}(p + \rho v^2) = 0 \\
&p = \frac{\rho}{\gamma}\left[1 + \frac{\gamma - 1}{2}(u^2 + v^2)\right]
\end{aligned} \tag{16}$$

These equations are the continuity equation, x and y direction momentum equations and the integrated form of the energy equation. The state variables in the equations are in a dimensionless form. The nondimensionalizing factors for the pressure, density and velocity components are, respectively, gamma times the free stream stagnation pressure, the stagnation density and the stagnation speed of sound.

The integration is started using the free stream values of the state variables as initial conditions. The state variables at the outer grid point are fixed at their free stream values. To satisfy the body boundary condition ($\vec{q} \cdot \nabla f = 0$), the normal component of velocity is treated as an odd function at the body. The sublayer value of the normal velocity component is set equal to the value at the first layer outside the body. The sublayer value of the remaining velocity component as well as pressure and density are determined using the reflection technique as used by Bohachevsky.[2] That is, the sublayer values are set equal to the corresponding values at one mesh point above the body. The integration starts at the second grid point (body) and proceeds to one point inside the outer grid point and in the x-direction from x = 1 to x = 2 at which point Kutler's stepback procedure is implemented.[4] The process is repeated until no further changes in the state variables occur.

Equations (6) were integrated using both Rusanov's and MacCormack's methods for a wedge with a 7.5° half-angle at a Mach No. of 2. Two mesh ratios were used. One at 1.272 which is near the experimental maximum for stability as determined by Kutler and the other at 1.0.[6] Three values of the free parameter, δ, associated with the Rusanov technique at a mesh ratio of 1.0 were used to evaluate the effect of δ on the solution.

Figure 11 shows the solution using Rusanov's method at the lower mesh ratio of 1.0 for δ values of 1.0, 2.0 and 3.0. The solution for a δ of 1.0 is distinctly inferior to those for δ's of 2.0 and 3.0 because of the excessive overshoots and undershoots in the vicinity

of the shock. The solution for $\delta = 2.0$ appears to yield a crisper shock than for $\delta = 3.0$ as well as lower-amplitude oscillations after the shock is encountered.

Figure 12 shows the solution using MacCormack's technique for $\Delta x/\Delta y = 1.0$. Although there is some overshoot from the shock layer side, the behavior for the free stream side is very good with no oscillations occurring.

Figures 13 and 14 show the results of using the Rusanov and MacCormack methods, respectively, at higher mesh ratios. The Rusanov free parameter, δ, was set equal to 3.0. While the MacCormack solution produces very little oscillation at the shock, the Rusanov solution exhibits excessive oscillations after the shock is encountered. However, running at a lower value of δ might decrease the oscillations shown in Fig. 11. Nevertheless, the shock crispness is about the same in both cases.

There is about a 30% saving in solution time using the MacCormack technique. Based on this fact and the results discussed above, it would appear that MacCormack's technique is superior for solving the wedge flow problem over the range of Mach numbers and wedge angles examined here.

Some additional experiments were performed using different coordinate systems to solve the wedge flow problem. One of these systems utilized distance along the wedge centerline and the tangent of the elevation angle as independent coordinates. Another was a pure polar system with radial distance and elevation angle as coordinates. Although the solutions in these coordinate systems are not reported here, they

proved to be satisfactory. The major difference noted was that computation times required to reach a solution were longer.

SHOCK REFLECTION PROBLEM

An additional example denoting the importance of the variation of local Courant number is provided by reflection of an oblique shock wave from a solid boundary. This is a well-defined problem in which the solution for the reflected shock angle and the downstream flow is uniquely determined by the downstream boundary condition. The solution is termed a regular reflection if the reflected shock is within the attached shock region for two-dimensional flow, and it is termed Mach reflection if the reflected shock angle is required by the downstream boundary condition to exceed the maximum allowable angle for an attached shock. The Mach reflection case is not of interest since the solution has an imbedded elliptic region within the flow field. The regular reflection case retains the hyperbolic character of the equations throughout the flow field.

The equations of motion in conservative form are

$$\begin{aligned} &\frac{\partial \rho u}{\partial x} + \frac{\partial \rho v}{\partial y} = 0 \\ &\frac{\partial (P + \rho u^2)}{\partial x} + \frac{\partial \rho uv}{\partial y} = 0 \\ &\frac{\partial \rho uv}{\partial x} + \frac{\partial (p + \rho v^2)}{\partial y} = 0 \end{aligned} \tag{17}$$

In addition, the energy equation is used in the form

$$\frac{\gamma}{\gamma - 1}\frac{p}{\rho} + \frac{u^2 + v^2}{2} = \frac{1}{\gamma - 1} \tag{18}$$

These equations are in nondimensional form with free stream stagnation values taken as the reference condition

$$\bar{p} = \frac{p}{\gamma p_{\infty T}} \quad , \quad \bar{\rho} = \frac{\rho}{\rho_{\infty T}} \quad , \quad \bar{u}, \ \bar{v} = \frac{u, \ v}{\sqrt{\frac{\gamma p_{\infty T}}{\rho_{\infty T}}}} \tag{19}$$

where the bar has been dropped in the nondimensional forms of the equations of motion. Both x and y have been nondimensionalized with respect to the same reference length.

The procedure used in obtaining a solution to the shock reflection problem is to initialize input conditions along an x = constant surface as shown in Fig. 15. Data input along this line are both pre- and post-shock values in the initial flow field. The integration then precedes step by step in the x direction as far as is desired. At the solid boundary (y = 0), reflection is used. That is the x-velocity component, pressure and density are taken to be even functions at the wall while the normal velocity component is assumed to be an odd function.

The x coordinate is assumed positive in the direction of the original free stream which is parallel to the wall. With this coordinate orientation, the maximum step size in the integration process is determined by the solution downstream of the reflected shock wave. In order to get a large variation in eigenvalues in the flow field, a set of initial conditions producing a shock close to the detachment region is important. This problem produces a more severe test of a differencing method than either the wedge or the solution of Burger's equation. The method must work well over a wide range of mesh ratios, and in addition must operate near the boundary where the character of the equations of motion changes from hyperbolic to elliptic. The wedge presents the same problem but is concerned with only one shock and two

regions of flow. It should be noted, however, that the influence of the mesh ratio size and the switch from hyperbolic to elliptic are really closely related. The maximum mesh size is determined by the maximum eigenvalue in the flow field and the equations of motion become elliptic when these eigenvalues become complex.

Figures 16-18 present results obtained with an original free stream Mach No. of 2 and an initial shock wave angle of 41° with respect to the free stream. The maximum allowable mesh ratio in each region is

$$\left(\frac{\Delta x}{\Delta y}\right)_{max} = \frac{u^2 - c^2}{|uv| + c\sqrt{u^2 + v^2 - c^2}} \tag{20}$$

Region I $\left(\frac{\Delta x}{\Delta y}\right)_{max} = 1.732$

II $\left(\frac{\Delta x}{\Delta y}\right)_{max} = 0.820$

III $\left(\frac{\Delta x}{\Delta y}\right)_{max} = 0.55$

The mesh ratio used was 0.375, approximately 70% of the maximum allowable for stability. The shock wave appears to be properly positioned for both techniques with Rusanov's method producing a shock wave spread over a greater number of mesh intervals. The most significant feature is the oscillatory nature of the solutions. The Rusanov $\delta = 3$ solution has several local oscillations while the large over and undershoot of MacCormack's method near the shock is undesirable. For this case, the Rusanov solution with $\delta = 2$ is clearly the most acceptable.

Figures 19-21 present similar data for a free stream Mach No. of 3. The mesh ratio range is

Region I $\left(\frac{\Delta x}{\Delta y}\right)_{max} = 2.83$

II $\left(\frac{\Delta x}{\Delta y}\right)_{max} = 0.78$

III $\left(\frac{\Delta x}{\Delta y}\right)_{max} = 0.35$

The same conclusions can be drawn regarding accuracy of solution as in the M = 2 case. One feature of interest is the apparent nonlinear limiting exhibited particularly by the Rusanov technique. The chopping of the crest on overshoot is a curious phenomena and one which the authors are at loss to explain at this time.

The Rusanov method produces the best results for the shock reflection study presented here as long as the delta parameter is below its limiting value of 3. The large overshoot of MacCormack's method and the local oscillations of Rusanov's method with $\delta = 3$ are undesirable for a problem of this type.

RECTANGULAR WING PROBLEM

The ultimate goal of the present study is to generate a numerical solution to the equations of motion describing the fluid flow about a rectangular wing. The solution of this problem really consists of three separate yet coupled individual studies. The first and most difficult is to determine the flow field generated about the leading edge and tips of the wing. The solution for the leading portion of the wing then forms the initial data plane for the second problem, calculation of the flow over the remainder of the wing. This in turn provides the initial data surface required to extend the solution downstream into the flow field.

The current status of this research is that solutions for the leading edge with three-dimensional tips have been obtained for the zero angle of attack case. The method of solution and resulting data is discussed in following sections.

The geometry of the leading edge portion of the assumed wing is shown in Fig. 22. The wing is really a wedge with half angle δ between the two tips followed by an afterbody. The geometry of the tips is such that the tip may be subsonic, i.e., lie within the Mach cone generated by the tip, or it may be supersonic. In addition, the tip is constrained geometrically to be conical in nature. That is, all points on the edge portion of the wing must be defined by an envelope of rays emanating from the tip.

The geometric constraints placed on the wing tip provide a conceptually straightforward way of solving for the flow field. Since the surface is conical in nature, the significant length dimension in the radial

direction is absent and the flow field is conical. This allows one to use the stepback procedure of Kutler in solving for the flow field.[4] It should be noted that the flow over the entire semi-span need not be computed since the flow over the wing between the tip Mach cones is two dimensional. The corresponding wedge flow solutions on the upper and lower surfaces then form the boundaries of the solution for the tip.

The exact geometry of the tip presumably could take any general conical form. The first problem studied here assumes that the tip is formed by a cone with the same half angle as the wedge portion of the wing. The second case is that of a flat end, i.e., the wedge abruptly terminates at the tip. These two problems are presented independently.

CONICAL TIP PROBLEM

Coordinate Systems

The tip geometry with a cone tip is presented in Fig. 23. The origin is at the tip with x measured downstream along the plane of symmetry, z is measured spanwise from the tip and y is normal to the plane of symmetry. The wedge and cone half angles are the same and are denoted by δ_w.

If the velocity components are u, v, and w, measured along the respective axes, the equations of motion in conservative form may be written

$$\begin{aligned}
&\frac{\partial \rho u}{\partial x} + \frac{\partial \rho v}{\partial y} + \frac{\partial \rho w}{\partial z} = 0 \\
&\frac{\partial (P + \rho u^2)}{\partial x} + \frac{\partial \rho uv}{\partial y} + \frac{\partial \rho uw}{\partial z} = 0 \\
&\frac{\partial \rho uv}{\partial x} + \frac{\partial (P + \rho v^2)}{\partial y} + \frac{\partial \rho vw}{\partial z} = 0 \\
&\frac{\partial \rho uw}{\partial x} + \frac{\partial (\rho vw)}{\partial y} + \frac{\partial (P + \rho w^2)}{\partial z} = 0
\end{aligned} \tag{21}$$

This set of equations is very convenient to use in obtaining finite difference solutions. However, specification of boundary conditions on the conical surface is cumbersome. The reason for this is that the body surface is not described by a constant coordinate such as x = constant. In this particular case the wedge surface is described by

$$y = x \tan \delta_w \tag{22}$$

while the cone is

$$\sqrt{y^2 + z^2} = x \tan \delta_w \tag{23}$$

It is advantageous to perform coordinate transformations on the equations of motion in order that the body surface be a constant coordinate surface. Since the geometry of the wedge and cone are quite different, two separate transformations must be used. This places a restriction on the coordinate systems in that they must meet smoothly at the interface, i.e., in the plane of juncture of the wedge and cone. This requirement provides identical mesh points in the interface plane and gives a smooth transition from the wedge to the cone.

Two coordinate systems satisfying this smooth transition were considered. The first is shown in Fig. 24. The transformation equations on the wedge for this system are really just a simple rotation given by

$$\begin{aligned} \xi &= x \cos \delta_w + y \sin \delta_w \\ \eta &= y \cos \delta_w - x \sin \delta_w \\ \zeta &= z \end{aligned} \tag{24}$$

The ξ coordinate is distance along the surface, η represents distance normal to the surface and $z = \zeta$ is spanwise distance as before. The smoothness requirement at the interface suggests that the tip transformations be such that ξ measure distance along the body, η represent distance normal to the cone and ζ denote the angle of rotation measured from the interface. The transformation equations are

$$\xi = \cos\ \delta w + \sqrt{y^2 + z^2}\ \sin\ \delta w$$

$$\eta = \sqrt{y^2 + z^2}\ \cos\ \delta w - x \sin\ \delta w \tag{25}$$

$$\zeta = \tan^{-1} \frac{z}{y}$$

The body surface equation for both the wedge and cone is just $\eta = 0$. This coordinate system has not been used although further investigation of its merit should be undertaken.

The second coordinate system considered is shown in Fig. 25. The transformation equations used on the wedge are

$$\xi = x$$

$$\eta = \frac{y}{x} \tag{26}$$

$$\zeta = z$$

The use of the tangent of the elevation angle, i.e., η rather than $\tan^{-1} \eta$ may or may not be advantageous. Since the coordinate is nonlinear, the resolution at the shock wave location is much finer than at the body. If this transformation is applied to an equation of the form

$$\frac{\partial E}{\partial x} + \frac{\partial F}{\partial y} + \frac{\partial G}{\partial z} = 0 \tag{27}$$

The result is

$$\frac{\partial \xi E}{\partial \xi} + \frac{\partial}{\partial \eta} (F - \eta E) + \frac{\partial \xi G}{\partial \zeta} = 0 \tag{28}$$

In this coordinate system the equations of motion become

$$\frac{\partial(\rho u\xi)}{\partial\xi} + \frac{\partial}{\partial\eta}(\rho v - \eta\rho u) + \frac{\partial(\rho w\xi)}{\partial\zeta} = 0$$

$$\frac{\partial\xi(P + \rho u^2)}{\partial\xi} + \frac{\partial}{\partial\eta}[\rho uv - \eta(P + \rho u^2)] + \frac{\partial}{\partial\zeta}(\rho uw\xi) = 0$$

$$\frac{\partial(\xi\rho uv)}{\partial\xi} + \frac{\partial}{\partial\eta}(P + \rho v^2 - \eta\rho uv\xi) + \frac{\partial}{\partial\zeta}(\rho vw\xi) = 0 \qquad (29)$$

$$\frac{\partial(\xi\rho uw)}{\partial\xi} + \frac{\partial}{\partial\eta}(\rho vw - \eta\rho uw) + \frac{\partial}{\partial\zeta}\xi(P + \rho w^2) = 0$$

The transformation equations required for the cone in order to proceed smoothly from the wedge to the cone are

$$\xi = x$$

$$\eta = \frac{\sqrt{y^2 + z^2}}{x} \qquad (30)$$

$$\zeta = \tan^{-1}\frac{z}{y}$$

The coordinates on the cone are analogous to those on the wedge. The only change is that ζ represents the angle measured from the interface plane outward toward the cone. The same difference in flow field resolution in the wedge transformation is observed here with η defined as a tangent.

Application of the transformation equations to general rectangular conservative form given by Eq. (27) results in

$$\frac{\partial\xi\eta E}{\partial\xi} + \frac{\partial}{\partial\eta}\left\{\eta[F\cos\zeta + G\sin\zeta - \eta E]\right\} + \frac{\partial}{\partial\zeta}[G\cos\zeta - F\sin\zeta] + \eta E = 0 \qquad (31)$$

The resulting conservation forms in the cone system become

$$\frac{\partial(\xi\eta\rho u)}{\partial\xi} + \frac{\partial}{\partial\eta}\left[\eta(\rho v\cos\zeta + \rho w\sin\zeta - \eta\rho u)\right]$$

$$+ \frac{\partial}{\partial\zeta}\left[\rho w\cos\zeta - \rho v\sin\zeta\right] + \eta\rho u = 0$$

$$\frac{\partial[\xi\eta(P + \rho u^2)]}{\partial\xi} + \frac{\partial}{\partial\eta}\left\{\eta\left[\rho uv\cos\zeta + \rho uw\sin\zeta - \eta(p + \rho u^2)\right]\right\}$$

$$+ \frac{\partial}{\partial\zeta}\left(\rho uw\cos\zeta - \rho vw\sin\zeta\right) + \eta(p + \rho u^2) = 0$$

$$\frac{\partial(\eta\xi\rho uv)}{\partial\xi} + \frac{\partial}{\partial\eta}\left\{\eta\left[(p + \rho v^2)\cos\zeta + \rho vw\sin\zeta - \eta\rho uv\right]\right\}$$

$$+ \frac{\partial}{\partial\zeta}\left[\rho vw\cos\zeta - (p + \rho v^2)\sin\zeta\right] + \eta\rho uv = 0$$

$$\frac{\partial(\xi\eta\rho uw)}{\partial\xi} + \frac{\partial}{\partial\eta}\left\{\eta\left[\rho uw\cos\zeta + (p + \rho w^2)\sin\zeta - \eta\rho uw\right]\right\}$$

$$+ \frac{\partial}{\partial\zeta}\left[(p + \rho w^2)\cos\zeta - \rho vw\sin\zeta\right] + \eta\rho uw = 0 \qquad (32)$$

These equations are somewhat complex and unwieldy to manipulate. It should be noted that the transformed equations pick up a nonhomogeneous term.

Equations (29) and (30) must be solved to obtain the flow field over the wing. These equations are a sort of hybrid set, in that the independent variables are pseudo-conical coordinates while the velocity components are measured in the positive direction of the original rectangular coordinate system. This feature insures that one can recapture the uniform free stream without using correction factors.[6]

Body Boundary Conditions

The boundary condition at the body surface provided by an analytic description of a problem of this nature is

$$\vec{q} \cdot \nabla F = 0 \tag{33}$$

where $\vec{q}$ is the velocity vector and F is the equation of the surface. Unfortunately, the numerical solution of such a problem cannot be completed with only this one condition.

The velocity vector is given by

$$\vec{q} = iu + jv + kw \tag{34}$$

and the scalar function, F, defining the surface of the wedge is given by

$$y - x \tan \delta_w = 0 \tag{35}$$

and by

$$\sqrt{y^2 + z^2} - x \tan \delta_w = 0 \tag{36}$$

for the cone. The boundary condition which is applicable to the wedge surface then becomes

$$v = u \tan \delta_w \tag{37}$$

which states that the body surface is a streamline in the flow. The condition on the cone surface is

$$u \tan \delta_w = v \cos \zeta + w \sin \zeta \tag{38}$$

Consider the wedge boundary condition. If one approximates the velocities at the body surface in terms of their values in the sublayer and the first mesh point above the surface, Eq. (37) may be written

$$\frac{v^+ + v^-}{2} = \frac{(u^+ + u^-)}{2} \tan \delta_w \tag{39}$$

This is a single equation in the two sublayer unknowns u^- and v^-. The process of reflection is used to provide the additional equations necessary to solve for the required sublayer values. This process is one in which the tangential velocity component and the scalar pressure and density are assumed to be even functions of the normal coordinate so their first derivatives vanish at the body surface. On the wedge surface the unit normal is given by

$$\vec{n} = \frac{\nabla F}{|\nabla F|} = - i \sin \delta_w + j \cos \delta_w \tag{40}$$

The tangential velocity is given by

$$\vec{q}_T = \vec{n} \times (\vec{q} \times \vec{n}) = i \cos \delta_w [u \cos \delta_w + v \sin \delta_w]$$

$$+ j \sin \delta_w [u \cos \delta_w + v \sin \delta_w] + k w \tag{41}$$

If the first derivative of the tangential velocity at the surface vanishes, then each component must vanish, i.e.

$$\begin{aligned} &\frac{\partial u}{\partial n} \cos \delta_w + \frac{\partial v}{\partial n} \sin \delta_w = 0 \\ &\frac{\partial w}{\partial n} = 0 \end{aligned} \tag{42}$$

notice that only two of the components provide useful information. If the derivatives are approximated to first order, then

$$w^+ = w^- \tag{43}$$

and

$$(u^+ - u^-) \cos \delta_w + (v^+ - v^-) \sin \delta_w = 0 \tag{44}$$

solving Eqs. (39) and (44) for u^- and v^-

$$u^- = \frac{u^+(1 - \tan^2\delta w) + 2V^+ \tan \delta w}{\sec^2\delta w}$$
$$v^- = (u^+ + u^-)\tan \delta w - v^+ \tag{45}$$

In addition, the normal derivatives of p and ρ are set equal to zero requiring that

$$p^- = p^+$$
$$\rho^- = \rho^+ \tag{46}$$

This provides a complete set of body surface boundary conditions for the wedge portion of the wing.

The boundary conditions for the cone are derived in the same fashion. The unit normal vector on the cone surface is

$$\vec{n} = \frac{\nabla F}{|\nabla F|} = - i \sin \delta w + j \cos \delta w \cos \zeta + k \cos \delta w \sin \zeta \tag{47}$$

and

$$\vec{q}_T = i[u \cos^2 \delta w + (v \cos \zeta + w \sin \zeta)\sin \delta w \cos \delta w]$$
$$+ j[u \sin \delta w \cos \delta w \cos \zeta + v(1 - \cos^2 \delta w \cos^2 \zeta)$$
$$- w \cos^2 \delta w \sin \zeta \cos \zeta] + k[u \sin \delta w \cos \delta w \sin \zeta$$
$$- V \cos^2 \delta w \sin \zeta \cos \zeta + w(1 - \cos^2\delta w \sin^2 \zeta)] \tag{48}$$

An approximate reflection of the tangential velocity can be obtained by equating the components of velocity parallel to the body surface in the sub and super layers. In vector form

$$\vec{n} \times (\vec{q} \times \vec{n}) = \vec{n} \times (\vec{q} \times \vec{n}) \tag{49}$$

The scalar forms are lengthy and are not presented. They will be included in a later, more complete report.

Only two of the components of Eq. (49) are independent as in the case of the wedge. If the normal velocity is set equal to zero as in Eq. (38) and any two of the components of Eq. (49) are differenced and solved for the sub layer values, the solutions are

$$u^- = u^+\left(\frac{1-\eta^2}{1+\eta^2}\right) + \frac{2\eta}{1+\eta^2}\left[v^+ \cos\zeta + w^+ \sin\zeta\right]$$

$$v^- = \frac{2\eta}{1+\eta^2}\,u^+ \cos\zeta + \frac{v^+}{1+\eta^2}\left(\eta^2 + \sin^2\zeta - \cos^2\zeta\right) - \frac{2w^+}{1+\eta^2}\cos\zeta \sin\zeta$$

$$w^- = \frac{2\eta}{1+\eta^2}\,u^+ \sin\zeta - \frac{2v^+}{1+\eta^2}\sin\zeta\cos\zeta \frac{+\,w^+}{1+\eta^2}\left(\eta^2+\cos^2\zeta - \sin^2\zeta\right) \tag{50}$$

The assumption has been made that the cone angle is small and this is at best an approximation of order 0 to the reflection.

The numerical solution of the equations of motion is obtained by initializing at all mesh points in a plane at a given distance from the leading edge, integrating to twice that distance, stepping back and repeating the procedure. Integration is carried out in a series of planes perpendicular to the ξ axis. The integration region in each plane is bounded by the body, the free stream and the two-dimensional flow field on the wedge outside the tip Mach cone. If the angle of attack is zero and the wing is symmetric, the flow variables are reflected across the plane of symmetry at the tip.

A solution of the leading edge problem with a cone tip has been obtained at a free stream Mach No. of 2 and zero angle of attack. The solution required seven stepbacks to converge using a mesh twenty points from the body out into the flow field and thirty points wide. Each

stepback required 160 planes and the solution required approximately 26 minutes on the Iowa State IBM 360-65. Convergence was assumed when the difference in pressure at each point for successive stepbacks changed less than 0.5%.

Figures 26-28 present distributions of pressure normal to the body surface at various lateral positions on the wedge and the cone. Starting from the two-dimensional wedge solution, the shock gradually moves in as the plane of symmetry is approached. Several points of interest should be noted. The linear stability theory indicates that the critical plane in the flow is the interface plane. The solution bears this out as the shock appears to be crisper at the interface. The oscillations in the normal distributions near the body surface are of great concern. At the present time it is suspected that better, more accurate boundary conditions are required on the cone surface in order to eliminate these waves.

It is of interest to compare the value of surface pressure at the plane of symmetry with that of an equivalent cone. A 7.5^{o} cone at a free stream Mach No. of 2 has a surface pressure of 0.105 which is about 8% below that predicted as shown in Fig. 28. The surface pressure in the finite wing case should be higher since the tip is bounded on both sides by a two-dimensional wedge flow at a higher pressure. Figure 29 shows the pressure distribution around the tip various distances out into the flow field. No unusual behavior is noted and the distributions are well behaved. Figure 30 presents the shock wave shape around the tip. The shape is again well behaved and no unusual properties have been noted. It is of interest to note that the shock wave angle for 7.5^{o} cone at a free stream Mach No. of 2 is approximately

30^{o}. The shock angle in the plane of symmetry is roughly 32^{o} which means that the cone shock angle would be approximately one mesh point closer to the body than the wing tip solution in the $\zeta = 90^{o}$ plane. This is consistent with the pressure data, i.e., the shock produced by the wing tip is stronger than the shock produced by a cone with the same half angle.

RECTANGULAR TIP PROBLEM

The geometry of the flat tip problem is shown in Fig. 31. The wedge forming the leading edge of the wing is abruptly terminated forming a flat tip 90° to the leading edge. This geometry conveniently allows the same coordinate system to be used in solving for the flow field both inboard and outboard of the tip. The coordinates as shown are distance along the axis of symmetry measured from the tip, the tangent of the elevation angle measured from the plane of symmetry and distance measured outward from the tip in the spanwise direction.

Each ξ = constant plane in which integration takes place is a domain divisable into rectangular regions. The first region is bounded by a free stream on three sides and the $\zeta = 0$ plane containing the wing tip forms the fourth side. The second and third regions are above and below the wing. They are bounded by the free stream, the ζ = constant surface outside the tip Mach cone in the two-dimensional flow region, the body surface and the $\zeta = 0$ plane. The integration is carried out in region one first and then regions two and three.

The simplicity of the coordinate system is evidenced by the ease with which boundary conditions can be applied. On the wedge surface, the boundary conditions enforced are given by Eqs. (43) and (44) which require the surface to be a stream line in the flow. The ζ component of the velocity is also reflected so that $w^+ = w^-$ on the wedge.

The boundary conditions enforced on the edge of the wing are particularly simple because the surface containing the tip is a constant coordinate plane namely $\zeta = 0$. Pure reflection across the end is used and

$$u^- = u^+ \qquad w^- = -w^+$$

$$p^- = p^+ \qquad v^- = v^+ \tag{51}$$

$$\rho^- = \rho^+$$

These two sets of boundary conditions constitute those required to solve the general square tip wing problem at angle of attack. If the angle of attack is zero, the integration is confined to the upper half plan and pure reflection is used as a boundary condition across the plane of symmetry.

No solutions to the three-dimensional wing problem have been completed to date using the technique described here. Instabilities appear to originate in the plane of symmetry and cause the solution to become unstable. The stability analysis based on evaluation of the maximum eigenvalue indicates that the maximum occurs in the plane of symmetry. For an equation

$$\frac{\partial \vec{u}}{\partial x} + [A] \frac{\partial \vec{u}}{\partial y} + [B] \frac{\partial \vec{u}}{\partial z} = 0 \tag{52}$$

under the transformation given by Eq. (26), the resulting form is

$$\frac{\partial \vec{u}}{\partial \xi} + \frac{[A] - \eta[I]}{\xi} \frac{\partial \vec{u}}{\partial \eta} + [B] \frac{\partial \vec{u}}{\partial \zeta} = 0 \tag{53}$$

The maximum eigenvalue of the matrix

$$\frac{[A] - \eta[I]}{\xi} \tag{54}$$

occurs in the plane where $\eta = 0$ and the maximum mesh size must thus be determined there. On the basis of this investigation and the behavior of the computer program it would appear that the mesh ratios used are too large, and instabilities occur as a result.

Another problem exists because of the square corner at the wing tip. Because the corner is square, a vortex may appear near the corner point even for the case where angle of attack is zero. At this time, sufficient data has not been obtained to understand this problem and its effect on the flow field. The corner is currently being treated as a sort of floating point. That is, it is defined within one mesh point. Reflection is used on the surface at all points except the corner point where these conditions are unnecessary. In this sense, the corner may not appear to be square but it is simply defined to be somewhere within a cell containing what has been referred to as the corner point.

INITIAL PROGRESS ON OPTIMUM COMPUTING METHODS

Some initial thought has been given to optimum computing methods and some initial progress has been made. Study and development of techniques in this area are an important part of work continuing under the extension of the present NASA grant.

Kutler and Lomax have noted that shock resolving ability of a finite difference technique can be improved by three methods: (a) increasing the order of the differencing scheme, (b) refining the mesh, and (c) adjusting the mesh on a local basis or adjust some system parameter so that the mesh is near the local characteristics.[10] The third idea is of interest in this study.

If a technique is adjusted so that the mesh is nearly coincident with the local characteristics, this means an effective local Courant number of one is desired. A difference method such as MacCormack's provides an exact solution at least in the linear case when the Courant number is unity. This is observed in the modified equation generated by use of the simple wave equation in an earlier section of this report (Eq. 11).

Local Mesh Changes

Present finite difference methods are applied holding the value of the mesh ratio at a fixed number throughout the solution of the problem. In the typical one-dimensional case, the mesh ratio is usually determined by the Courant-Lewy-Friedrick's stability criterion, which reads

$$\left| \sigma_{max} \frac{\Delta T}{\Delta x} \right| \leq 1 \tag{55}$$

where σ_{max} is the maximum eigenvalue of the hyperbolic system and $\Delta T/\Delta x$ is the mesh ratio. The use of this as a method of establishing mesh size is based upon a linearized stability analysis. The stability boundary is reached (at least in the linear case) if the local step size or mesh ratio is set equal to the reciprocal of the maximum eigenvalue of the system. It may be shown that if calculations are carried out at the maximum mesh ratio or at the shift condition, the mesh is then compatible with the local characteristics.

The most convenient model of inviscid fluid equations is again the modified Burger equation used to develop numerical techniques operating at a local Courant number of one. Notice again that this equation retains the nonlinear character of those describing fluid flow.

Consider a simple Lax first-order technique applied to Burger's equation. The differenced form is

$$u_j^{n+1} = \left(\frac{u_{j+1} + u_{j-1}}{2} \right) - \frac{\Delta T}{2\Delta x} \left(\frac{u_{j+1}^2 - u_{j-1}^2}{2} \right) \tag{56}$$

The Lax method is used for simplicity. The ideas and applicability of the technique should not depend upon the differencing method. The usual stability requirement applied to Burger's equation becomes

$$\left| u_{max} \frac{\Delta T}{\Delta x} \right| \leq 1 \tag{57}$$

Suppose the local mesh ratio $\Delta T/\Delta x$ is varied according to the requirement

$$\frac{\Delta T}{\Delta x} = \left| \frac{1}{u} \right| \tag{58}$$

This requires that the local Courant number be one. The question must now be answered as to how this moves discrete data or how this propagates a discontinuity.

If Eq. (58) is substituted into Eq. (56) one obtains

$$u_j^{n+1} = \frac{u_{j+1}^n + u_{j-1}^n}{2} \left[\frac{2|u_j| - u_{j+1} + u_{j-1}}{2|u_j|} \right] \tag{59}$$

In addition to substituting for the local mesh ratio, the step size at that particular point in space and time must be altered. Assume that alterations in mesh ratio $\Delta T/\Delta x$ are achieved by changing ΔT while the x-grid is fixed in space. This means that after the initial step at $t = 0$, each value will have advanced a different amount in time. Suppose this is represented by the x-t plane shown in Fig. 32.

The time advance of the solution must be recorded at each step just as the x position is normally noted. The procedure used is to note the value of u at the jth point, set the time advance $\Delta T = |u_j^n| \Delta T$ and compute the value of u_j^{n+1} at $(t + \Delta t)_{local}$ using Eq. (9).

Since this method uses central differences, one chooses points for which values of u at $j - 1$ and $j + 1$ have advanced farther in time. In this way, values of u_{j+1}^n and u_{j-1}^n at the proper time can be deduced by interpolation.

A similar operating sequence is obtained by approximating $|u_j|$ by $|u_{j+1} + u_{j-1}|/2$ which is consistent with the Lax method. In this case, for u = positive, the difference equation reduces to

$$u_j^{n+1} = u_j^n \tag{60}$$

which is just a shift in time for each value at x. The time shift is given by

$$\Delta T = \frac{2\Delta x}{|u_{j+1} + u_{j-1}|} \tag{61}$$

These methods appear to be particularly simple and straightforward. Such is not the case. The difficulty is that wave propagation velocities are wrong. This can easily be seen by considering a square wave with $u_i = 0$ and $u_F = 1$. If a local time step is used in the $u_1 = 0$ range based upon $\Delta T = \Delta x/|u_j|$ it would appear that the value of u_j is the same for all time. In fact, one may state that local mesh altering on this basis distorts the wave speed at the leading edge of discontinuities. It becomes apparent that alterations of the mesh in both space and time are required to accurately track changes in the flow field. One must question the use of Eulerian methods if the mesh alterations become too complex. In essence, one is forced to track discontinuities in a finite mesh by altering the mesh so that it effectively moves with the wave fronts.

The fact that wave propagation speeds are wrong in time dependent flows indicates that one must be careful in using the method and interpreting the results. One place where this type of method can be and has been used is in solving the wedge flow equations. The wedge flow equations were solved as part of the preliminary investigation of this technique. Since the radial distance plays the analog of time, the advance is in the radial direction. The final answer is independent of radial distance so that phase errors in time or radial

distance are unimportant if a steady solution is sought. The only critical point is if the local eigenvalues in the flow go to zero. Results show that solutions obtained through variable mesh ratio are better although not significantly different from the fixed mesh results.

A wedge flow solution using the variable mesh ratio scheme was obtained by using the polar version of the equations of motion for wedge flow. The solution of the wedge flow equations using a Lax differencing method was used for initial data. Along each ray the local eigenvalue was calculated at a radius r = 1. Using this eigenvalue structure, a single integration step was taken and all variables were stepped back to r = 1 again. This method was used as opposed to a search for the minimum radius point due to long computing times required.

The first method used was to switch to an optimized Lax method after the original constant mesh Lax solution had converged. The change in solution produced was negligible and the results are not presented here. One must ask why much better results were not obtained. The reason must lie in the structure of the modified equations for the Lax method applied to wedge flow. Even though a mesh ratio is selected in such a way that the local Courant number is unity, the solution is really that of the modified equations and would be exact only on a locally linear basis.

More encouraging results have been obtained using second-order predictor-corrector methods. MacCormack's method was used as the difference approximation for the locally optimum method and the results are presented in Fig. 33. The results are not greatly different from

the standard fixed mesh method, but the locally optimum technique does produce the expected behavior at the shock. Oscillations appear on both sides of the shock. This leads one to speculate that the preferential nature of the method begins to look more like a central difference scheme.

The predictor-corrector roles were then reversed, i.e., backward prediction-forward correction, and a solution was computed. This is shown in Fig. 33. It is interesting to note that this produces very nearly the same result as the MacCormack technique. The reason again must reside in the fact that the modified equations for the two methods must be nearly the same; for the linear wave equation, the modified equations are the same. It would be an interesting experiment to see if the Lax-Wendroff method produces similar results.

Not enough mesh points were used to properly define the free stream in this case. Additional experiments are planned and this problem will be avoided.

Free Parameter Methods

Several attempts at modifying differencing methods have been made by including a separate parameter that can be adjusted independently of the mesh size. Typical of these is the Rusanov method[6] and more recently that proposed by Kutler and Lomax.[10] These methods are not based upon operating at the optimum Courant number; they instead pose the question: given a fixed mesh size, is there a value of the free parameter which gives the best solution for that mesh ratio? The term

"best solution" at least in the linear case is taken to mean that solution for which the shift condition is most nearly satisfied.

The accuracy of a given technique applied to a specific equation is best determined by examining the resulting modified equation. Specifically, the Rusanov method applied to the linear wave equation produces modified Eq. (14). At the design point, i.e., $\nu = 1$, $\delta = 3$ the shift condition is satisfied and the solution of the wave equation is exact. If one is operating off design, the right-hand side of the equation must be minimized.

This poses a minimization problem in which several constraints must be observed. In this case, the wave speed, c, the Courant number, ν, and the mesh size, Δx, are fixed, along with the derivatives at a given x position. The only parameter that can be varied is δ and this can vary only within the stability bounds of the method. The first thought is to simply set the coefficient of the fourth derivative term equal to zero. This yields

$$\delta = \frac{4\nu^2 - \nu^4}{3}$$

clearly outside the linear stability bound. The same result occurs if the fifth derivative coefficient is set equal to zero.

The parameter δ is free to vary with ν, x, and t. If only the fourth derivative term is considered the problem is one in which one must find

$$\text{MIN}\left|\left(\frac{3\delta}{\nu} - 4\nu + \nu^3\right)u_{xxxx}\right| = \text{MIN}\left|F(\nu, x, t)\right| \qquad (62)$$

subject to the stability constraints of the system. This is a minimization problem in three independent variables ν, x and t. It should yield to standard minimization techniques. The difficulty is that some approximation for the spatial derivative of u is required. This results in more complexity, storage and computer time required when δ is calculated.

At this time, proceeding along these lines does not look very promising. The main difficulty is presented by the complex structure of the modified equation. The alternative is to perform numerical experiments which would provide at least a qualitative answer as to what value of the δ parameter should be used. Unfortunately, the numerical experiment approach does not provide a general technique nor does it present insight into the reasons for selecting a given δ.

It is anticipated that some effort will continue to be expended in considering free parameter methods. However, it appears that less restrictive techniques which use the free parameter approach should lend themselves to easier analysis.

FUTURE PLANS

The first priority in the continued research effort is to obtain additional solutions for the cone tip wing problem. A study of the effect of altering the surface boundary conditions on the cone is imperative. The oscillations in the flow variables near the body are of great concern and perhaps better boundary conditions will eliminate this problem. Kutler's results indicate that better surface boundary conditions may eliminate these oscillations. Both the MacCormack method and the third-order Rusanov technique will be used on this problem at zero and nonzero angle of attack.

Additional effort will be expended in obtaining a solution for the rectangular wing with a flat or squared tip. The program for this problem using MacCormack's method is complete and in the de-bug stage. Difficulties are being experienced with stability near the plane of symmetry of the wing. The linear stability analysis indicates that this is the critical surface in the flow and in fact attempts to obtain solutions diverge in this plane. It appears that a more careful assessment of the stability requirements for this problem must be made.

A solution continuing downstream over the wing and in the afterflow will be sought. The initial conditions for this problem are supplied by solution of the leading edge problem. Since this is an initial value problem, no difficulties are anticipated in implementing techniques to complete its solution. The selection of the body shape is undecided at present. Current plans are to use either a power law extension after the wedge to the trailing edge or to use a simple double wedge configuration. The downstream solution past the trailing

edge of the wing is again a simple initial value problem and no difficulties are expected.

Pending completion of the rectangular wing problem, work proposed for the continuation of this grant on the pyramid-shaped body will begin. As noted in this report, proposed work on optimum differencing methods has started and will be continued.

One additional project will be initiated. This investigation will be concerned with the relative accuracy of solutions obtained by differencing the original equations in conservative form or in the advective form. Most applications in gas dynamics have been made using the conservative form while the meteorologists particularly favor the advective form of the equations of motion. It is hoped that this study will provide insight into the advantages and disadvantages of each way of differencing.

REPORTS AND PUBLICATIONS

Although no publications have been produced during the first year, plans include release of several reports during the next six months. A detailed report including comprehensive results obtained with Burger's equation, wedge flow and shock reflection from a solid boundary is currently under preparation and will be completed during the next two or three months. The final report on research on the finite thickness rectangular wing will be published sometime during the coming year. Present plans are to finish that phase of the research effort by November at which time the final report will be written. It is anticipated that a report on conservative versus advective differencing will be completed within the next six months. This work is to be completed by a graduate assistant in research and should be finished by November.

REFERENCES

1. Bohachevsky, I. O., and Rubin, E. L., "A Direct Method for Computation of Nonequilibrium Flows with Detached Shock Waves," AIAA J., 4: 600-607 (1966).

2. Bohachevsky, I. O., and Mates, R. E., "A Direct Method for Calculation of Flow about an Axisymmetric Blunt Body at Angle of Attack," AIAA J., 4: 776-782 (1966).

3. DeJarnette, F. R., "Application of Lax's Finite Difference Method to Nonequilibrium Hypersonic Flow Problems," NASA Technical Report R-234 (1966).

4. Kutler, P. K., "Application of Selected Finite Difference Techniques to the Solution of Conical Flow Problems," PhD Thesis, Iowa State University, Ames, Iowa (1969).

5. MacCormack, R. W., "The Effect of Viscosity in Hypervelocity Impact Cratering," AIAA Paper No. 69-354: 1-7 (1969).

6. Rusanov, V. V., "On Difference Schemes of Third-Order Accuracy for Nonlinear Hyperbolic Systems," J. Computational Phys. 5: 507-516 (1970).

7. Lax, P. D., "Weak Solutions of Nonlinear Hyperbolic Equations and their Numerical Computation," Comm. Pure Appl. Math., 7: 159-193 (1954).

8. Burstein, S. Z., and Mirin, A. A., "Third Order Difference Methods for Hyperbolic Equations," J. Computational Phys., 5: 547-571 (1970).

9. Hopf, E., "The Partial Differential Equation $u_t + uu_x = \mu u_{xx}$, Comm. Pure Appl. Math., 3: 201-230 (1950).

10. Kutler, P., and Lomax, H., "The Computation of Supersonic Flow Fields about Wing-Body Combinations by 'Shock Capturing' Finite Difference Techniques," Ch. 8, Lecture Notes in Physics, Springer Verlag (1971).

11. Richtmeyer, R. D., and Morton, K. W., Difference Methods for Initial Value Problems, John Wiley and Sons, Inc.: New York, N.Y. (1967).

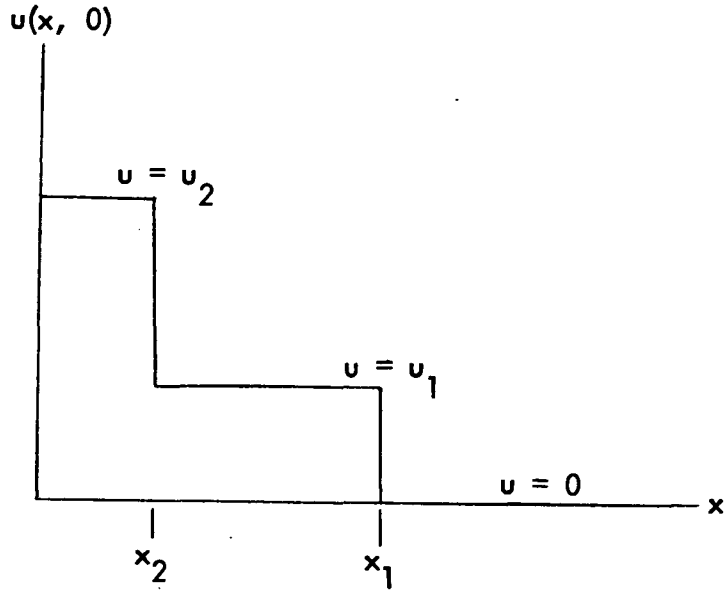

Fig. 1. Initial conditions for Burger's equation.

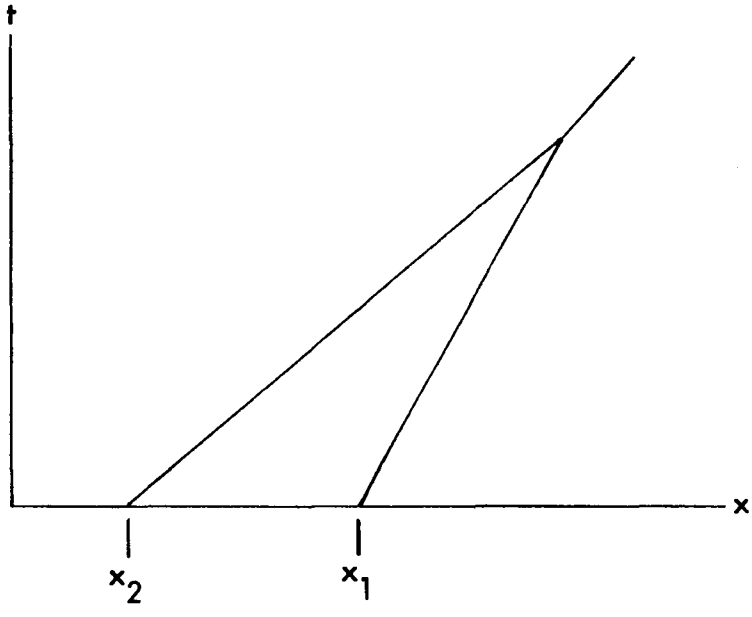

Fig. 2. Space-time solution for overtaking discontinuities.

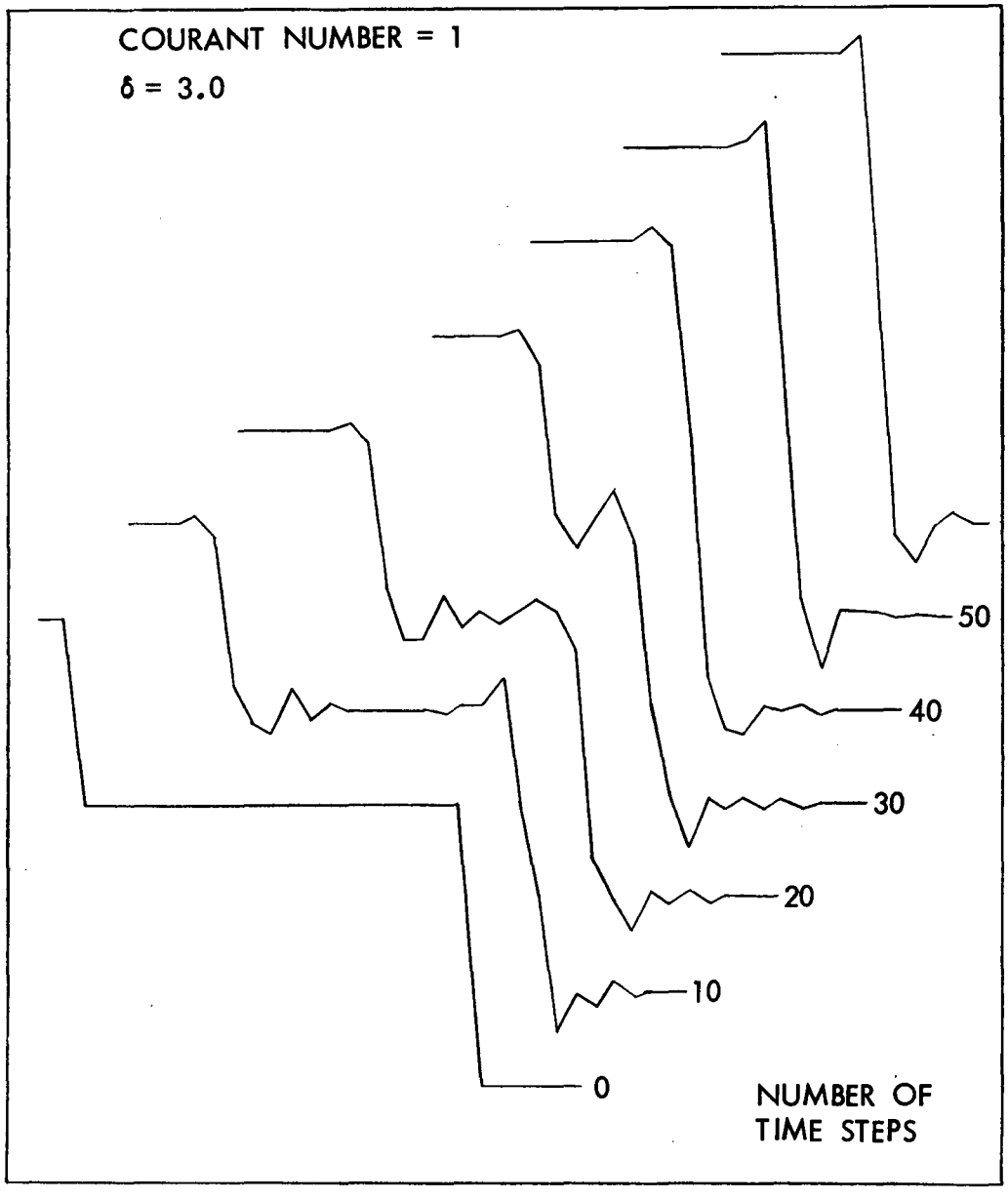

Fig. 3. Burger's equation solution, Rusanov method.

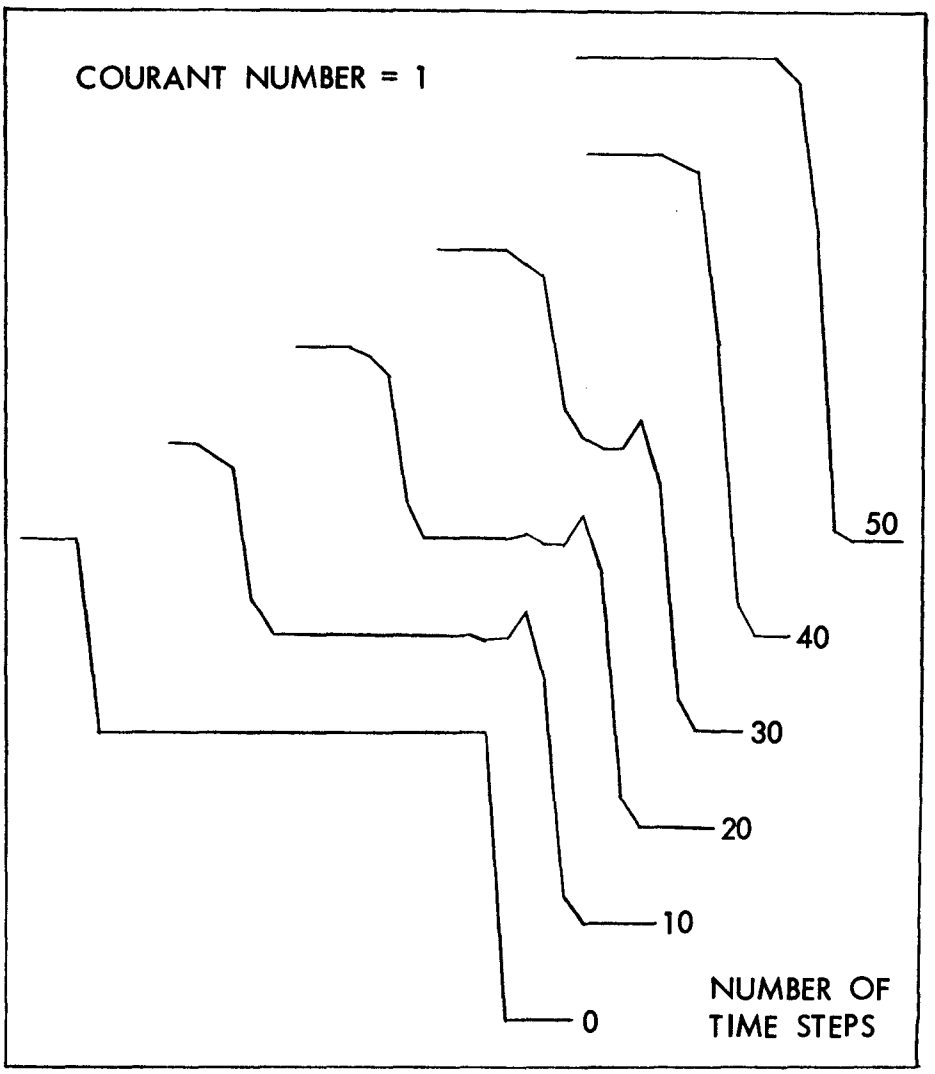

Fig. 4. Burger's equation solution, MacCormack method.

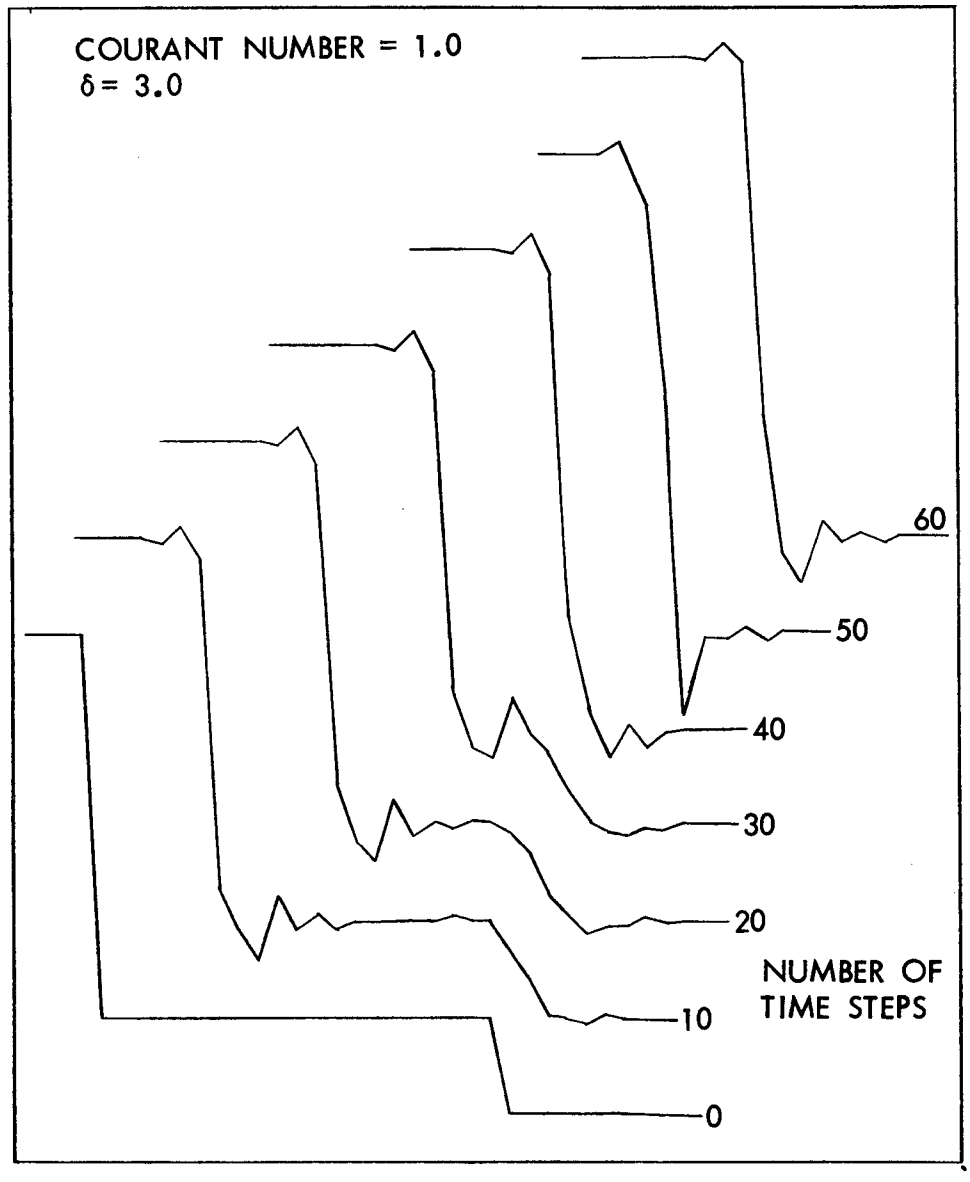

Fig. 5. Burger's equation solution, Rusanov technique.

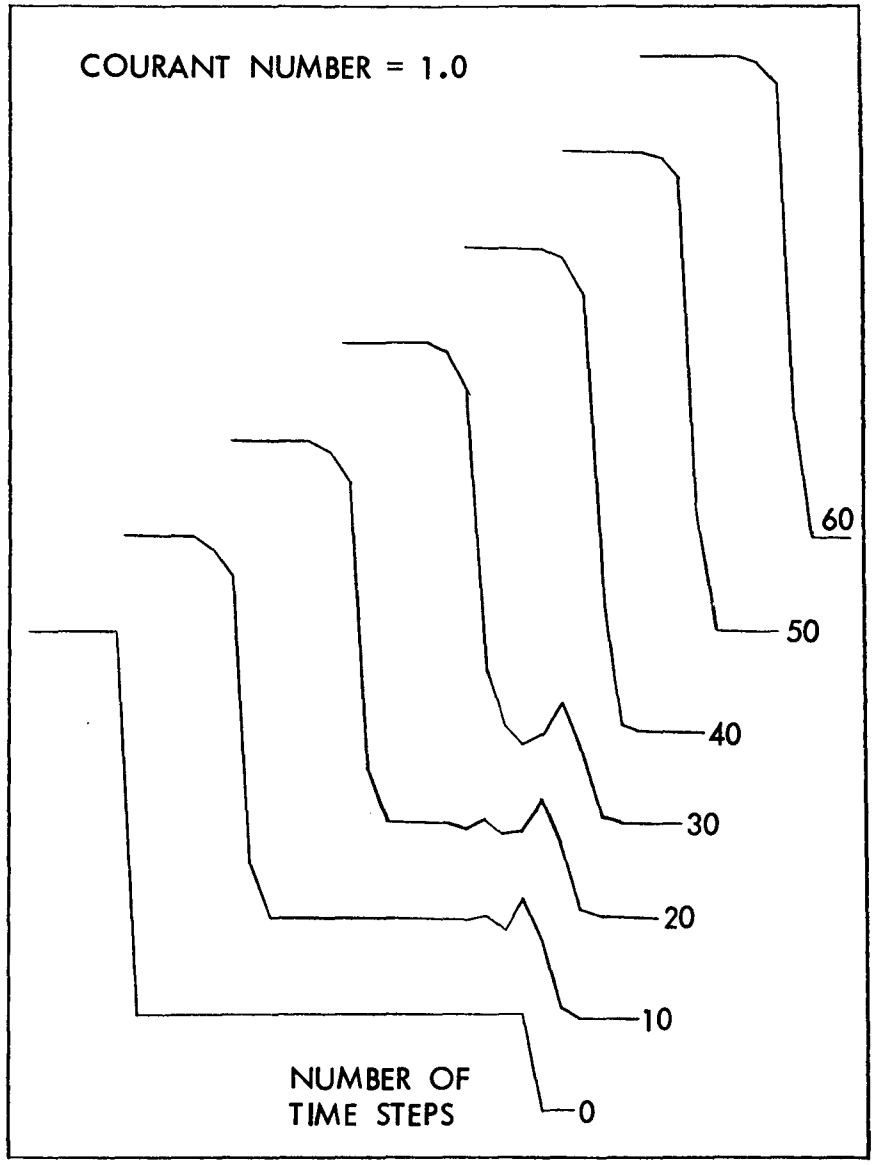

Fig. 6. Burger's equation solution, MacCormack technique.

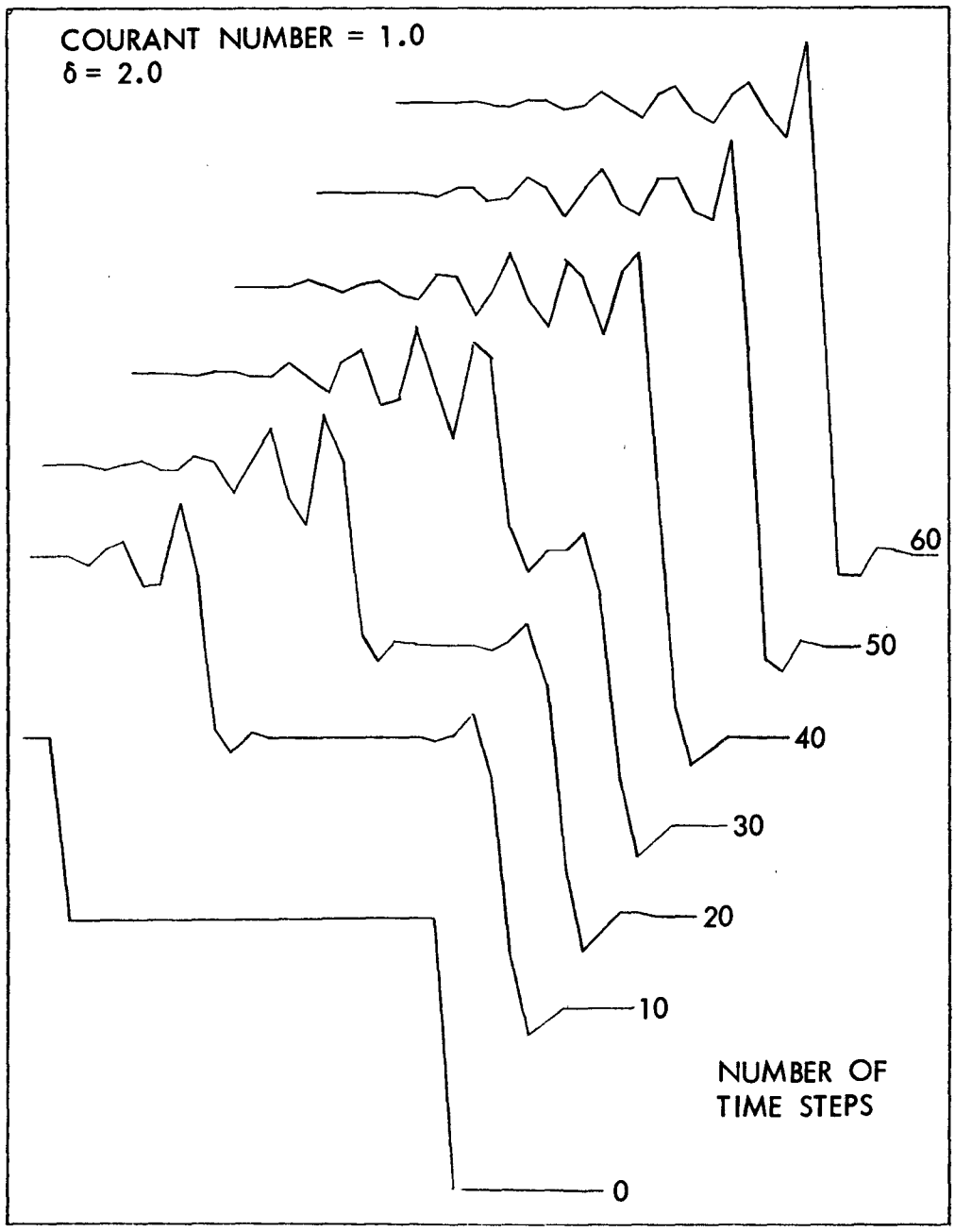

Fig. 7. Burger's equation solution, Rusanov technique.

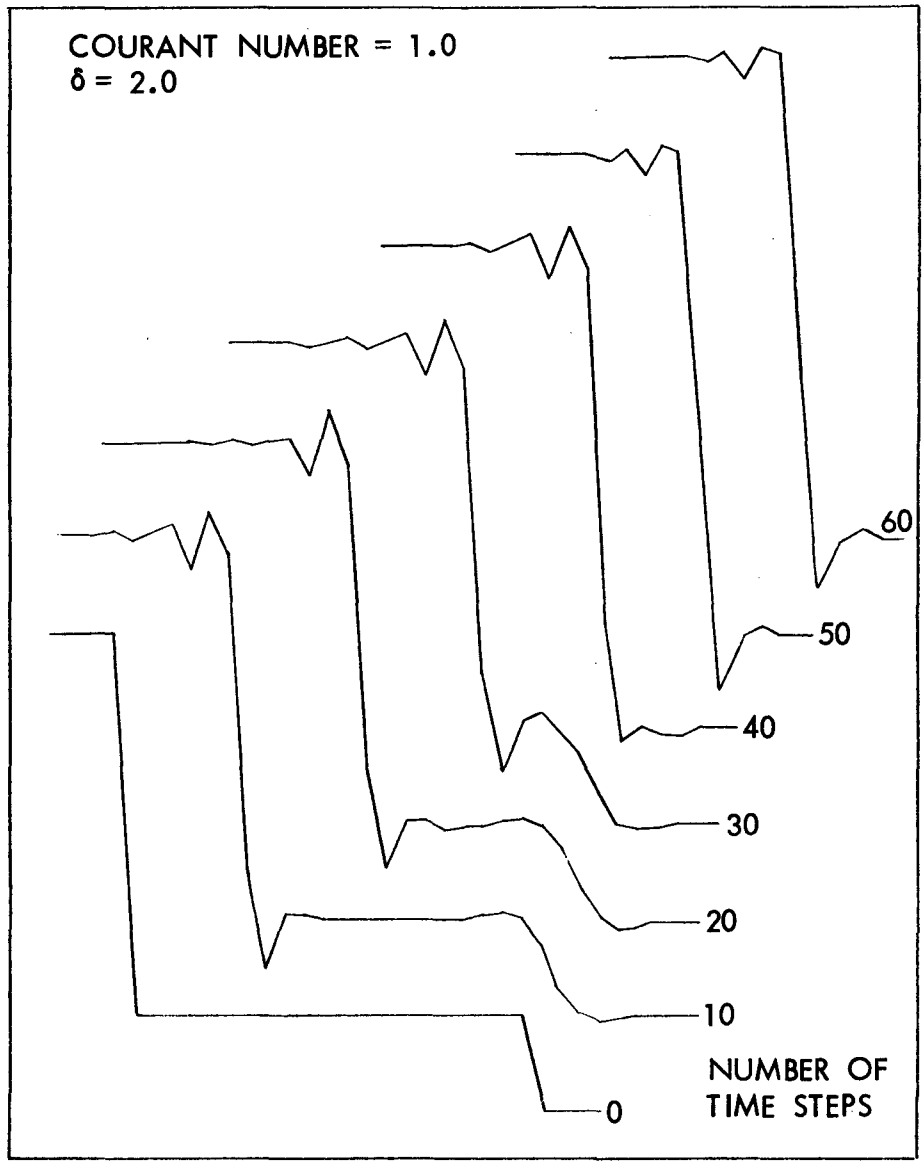

Fig. 8. Burger's equation solution, Rusanov technique.

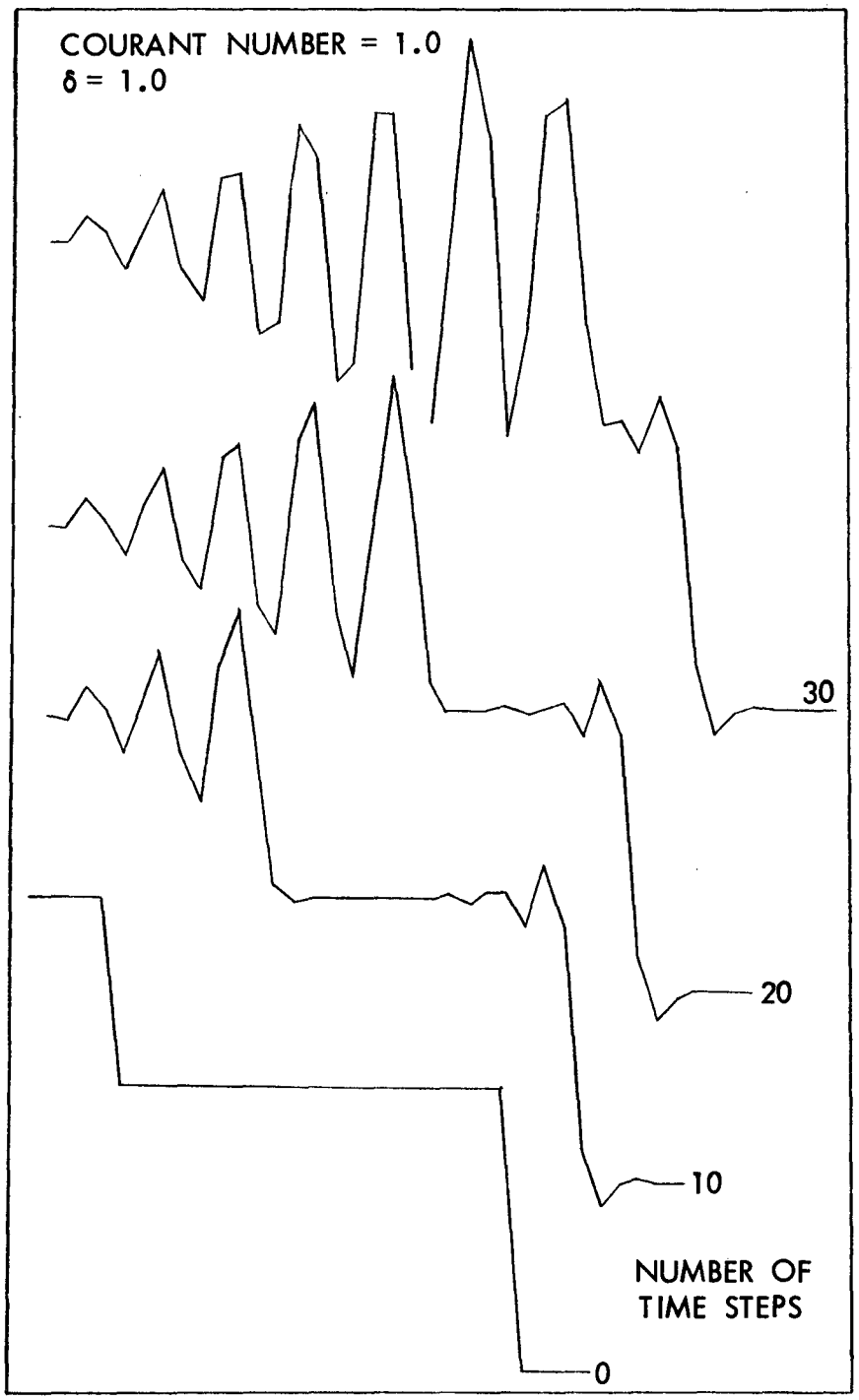

Fig. 9. Burger's equation solution, Rusanov technique.

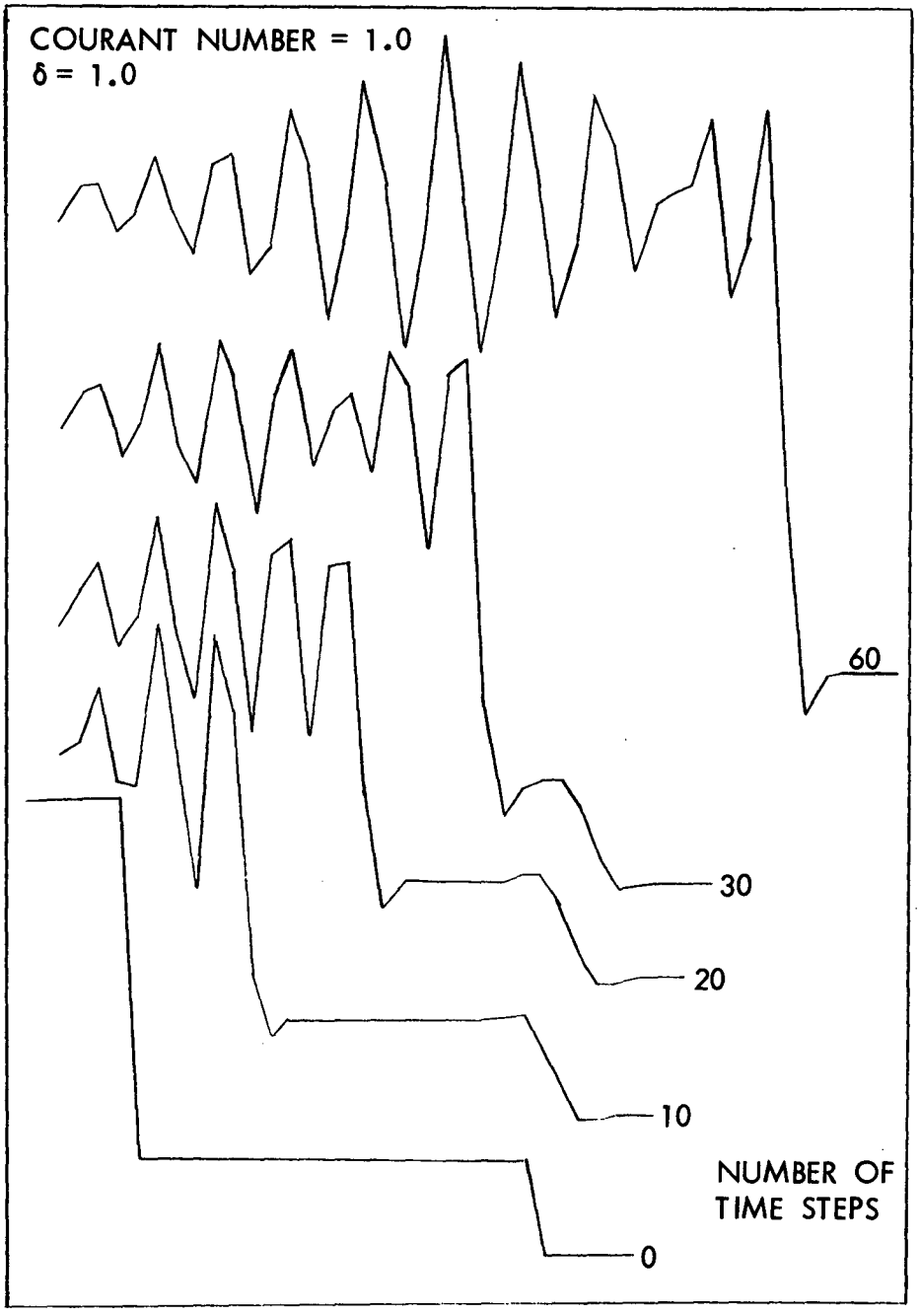

Fig. 10. Burger's equation solution, Rusanov technique.

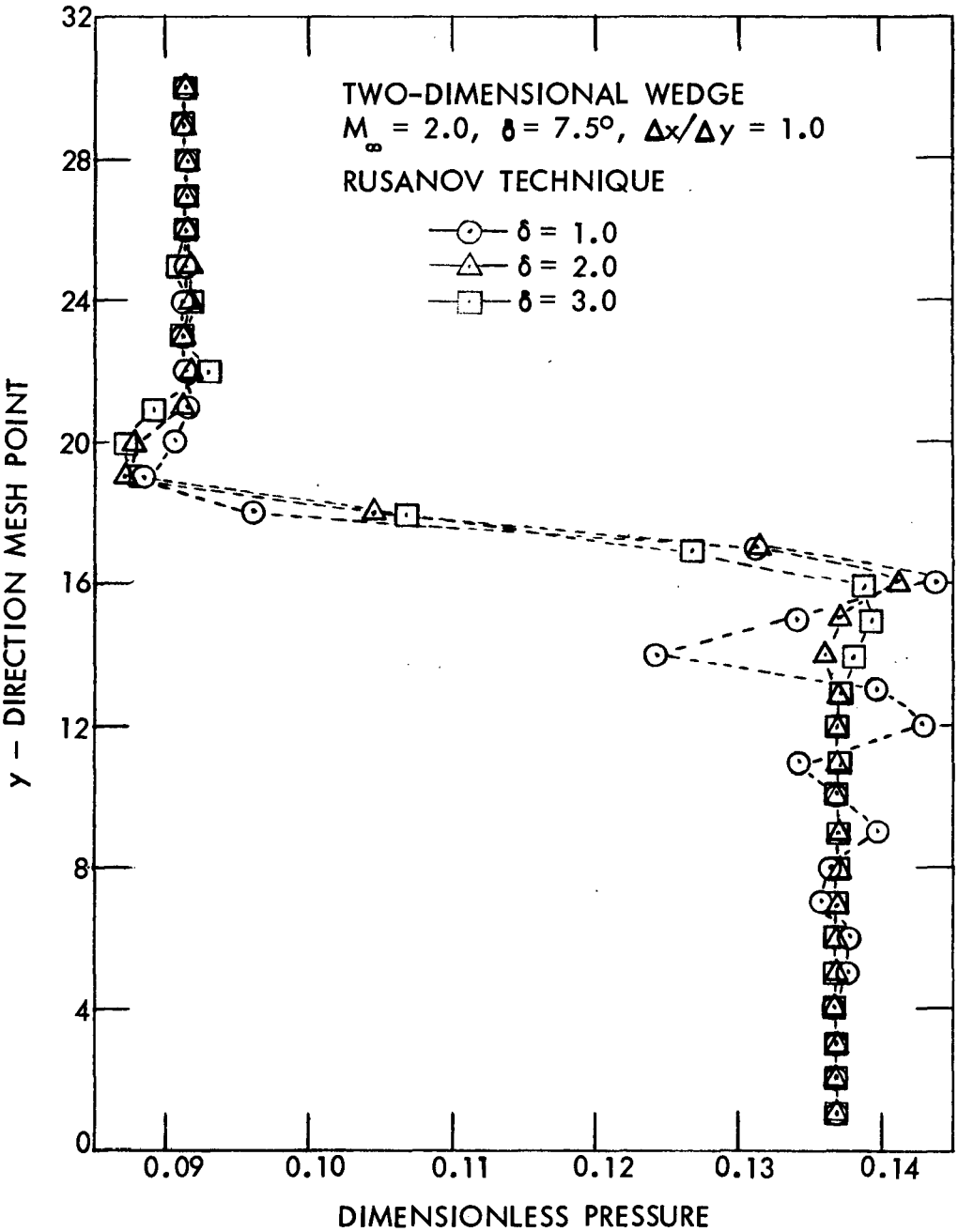

Fig. 11. Pressure distribution in a direction normal to wedge surface.

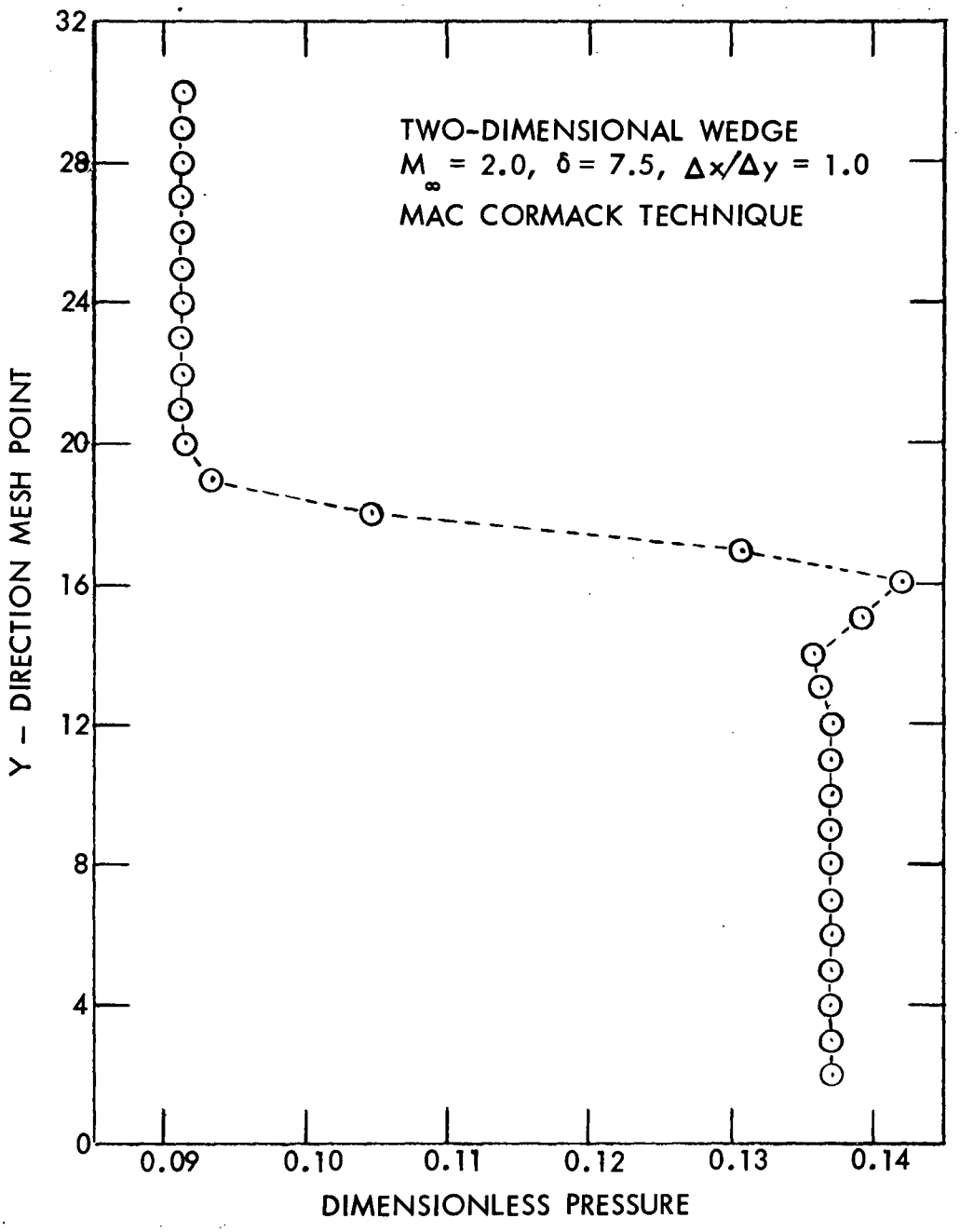

Fig. 12. Pressure distribution in a direction normal to wedge surface.

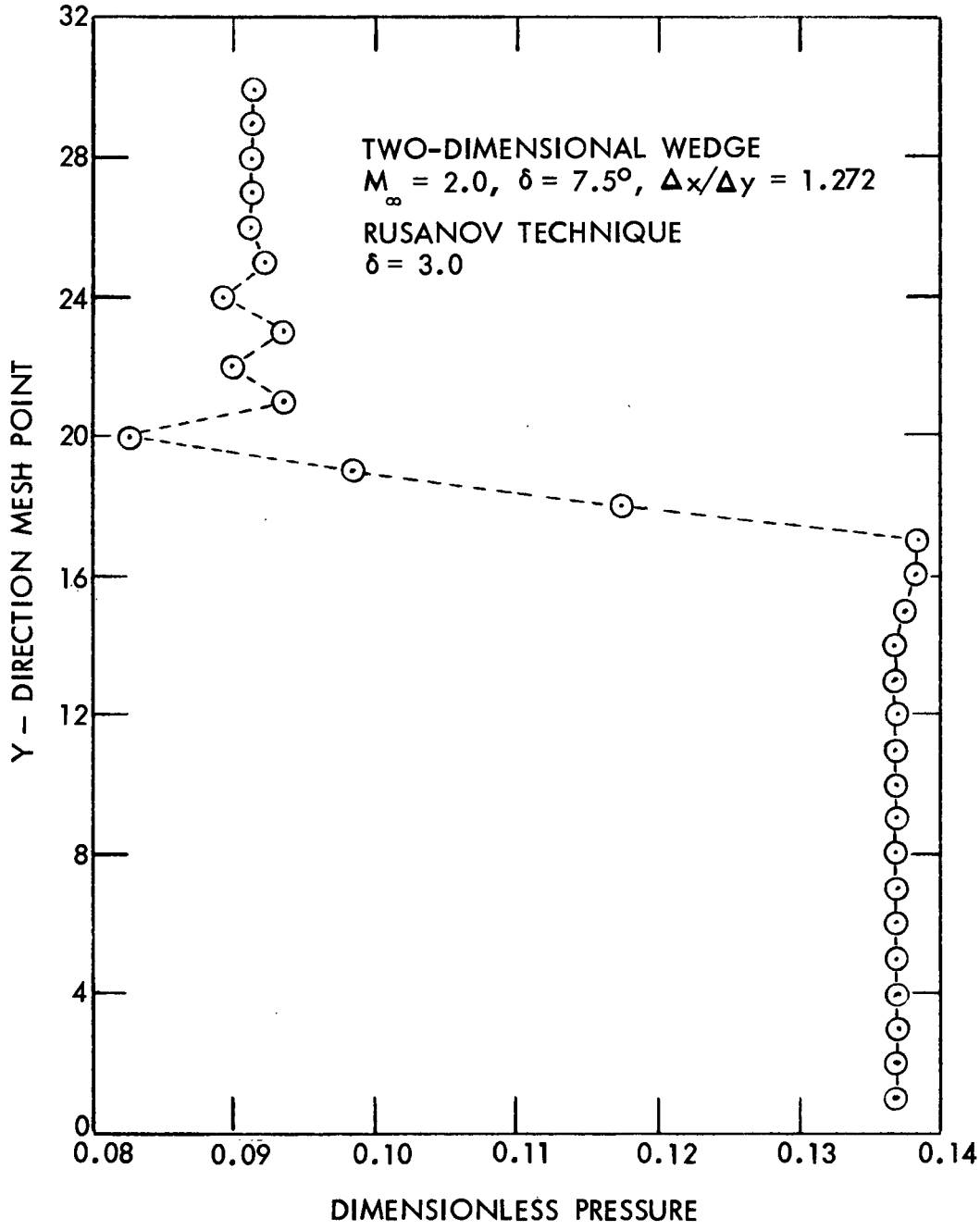

Fig. 13. Pressure distribution in a direction normal to wedge surface.

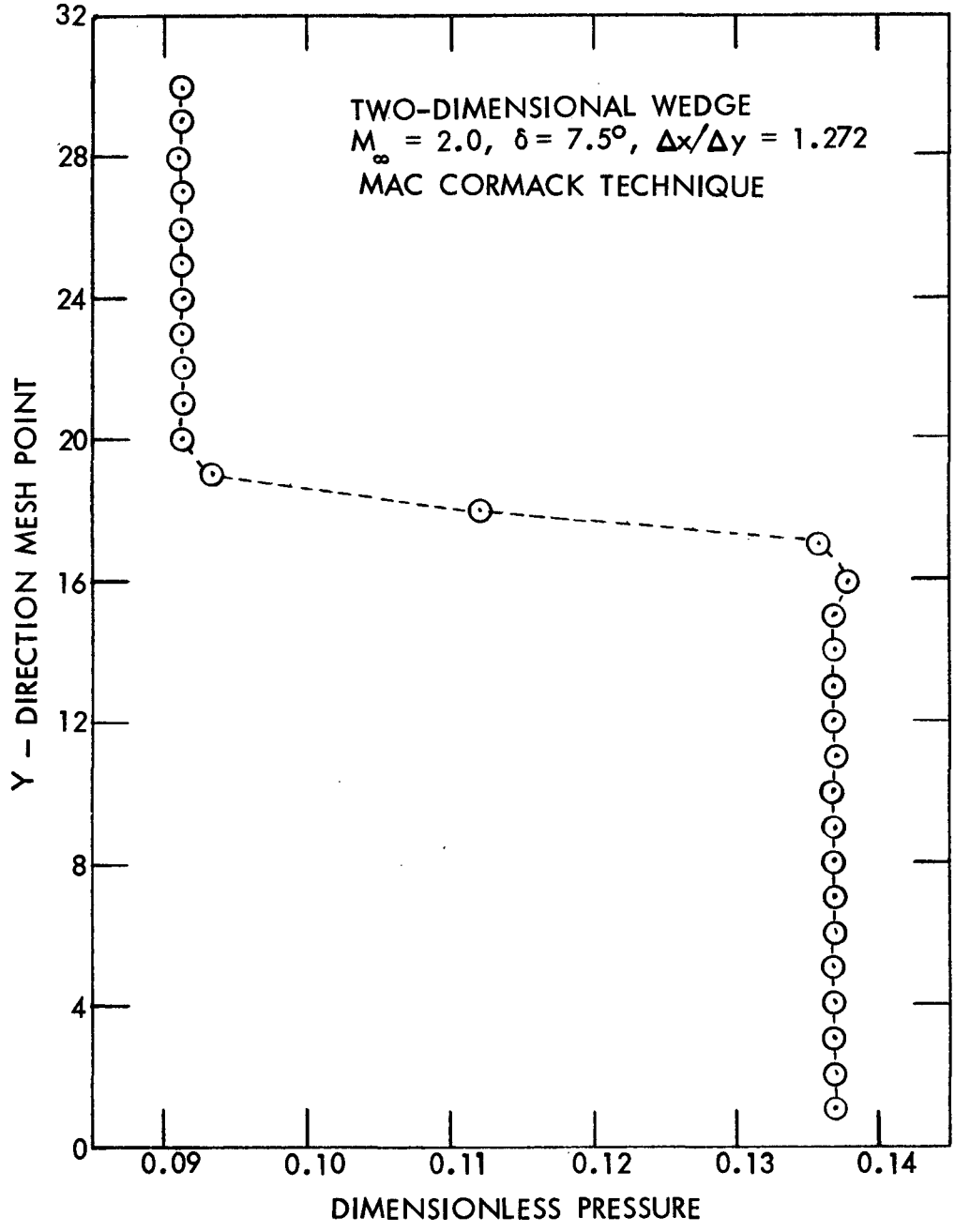

Fig. 14. Pressure distribution in a direction normal to wedge surface.

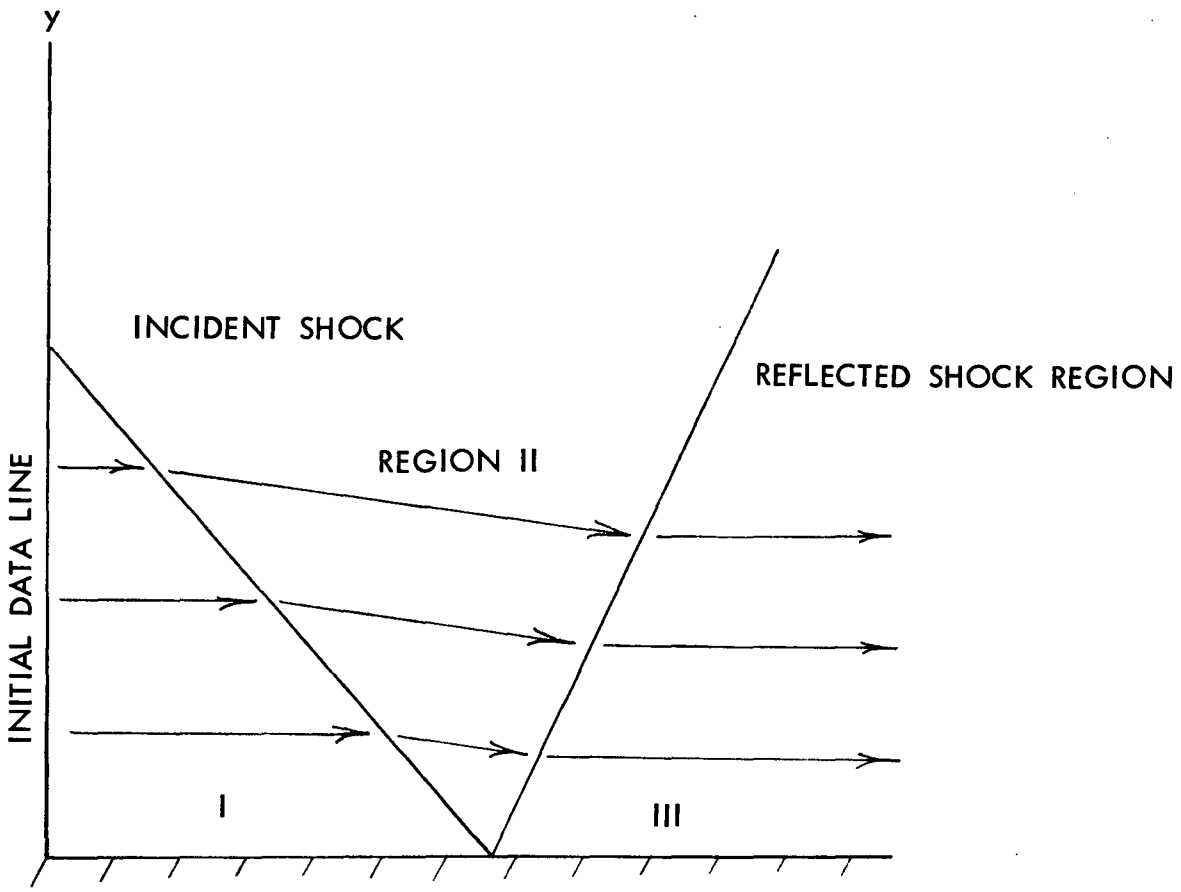

Fig. 15. Shock reflection geometry.

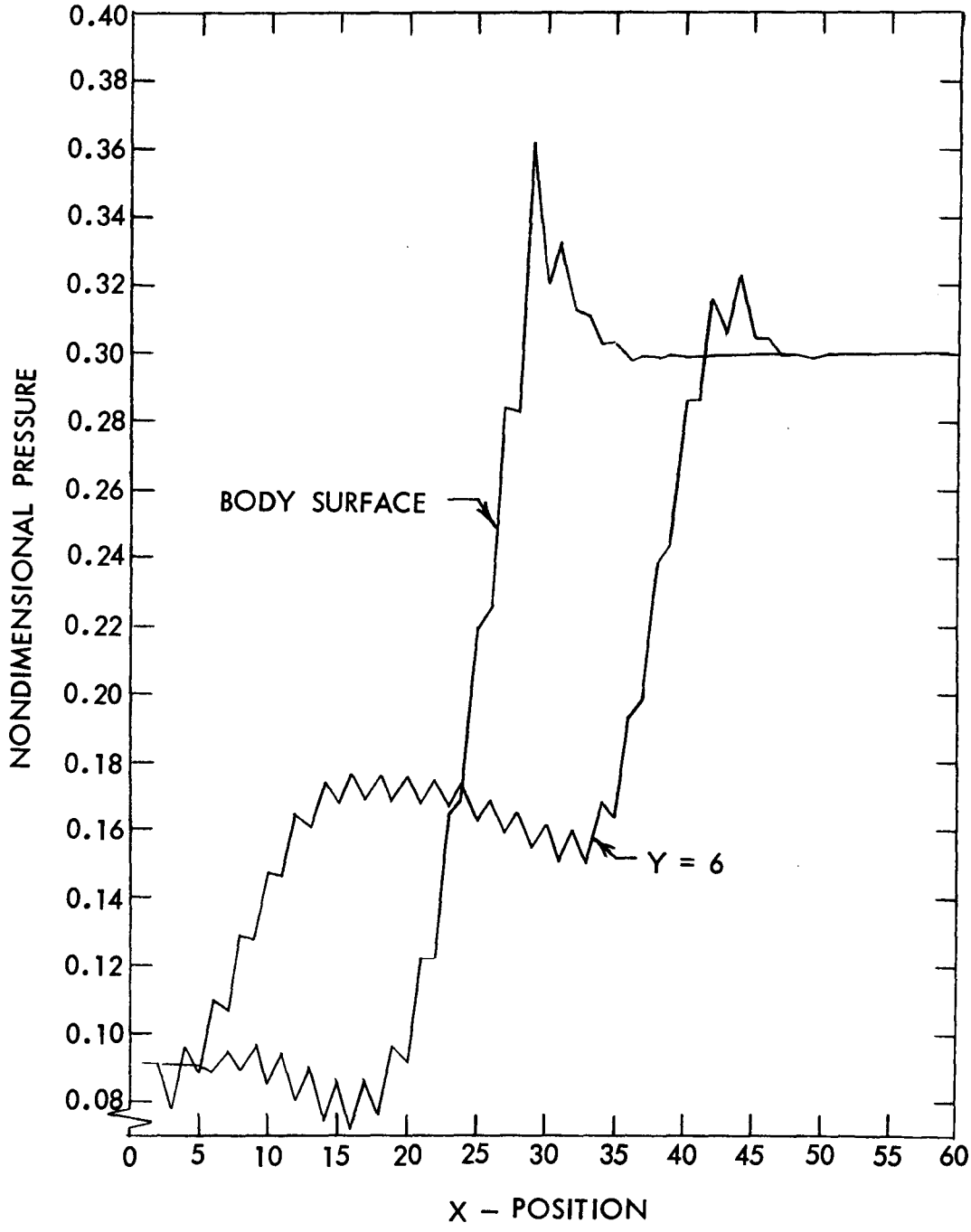

Fig. 16. Shock reflection, Rusanov method, $\Delta x/\Delta y = 0.375$, $\delta = 3.0$, $M = 2.0$, $\theta_s = 41^\circ$.

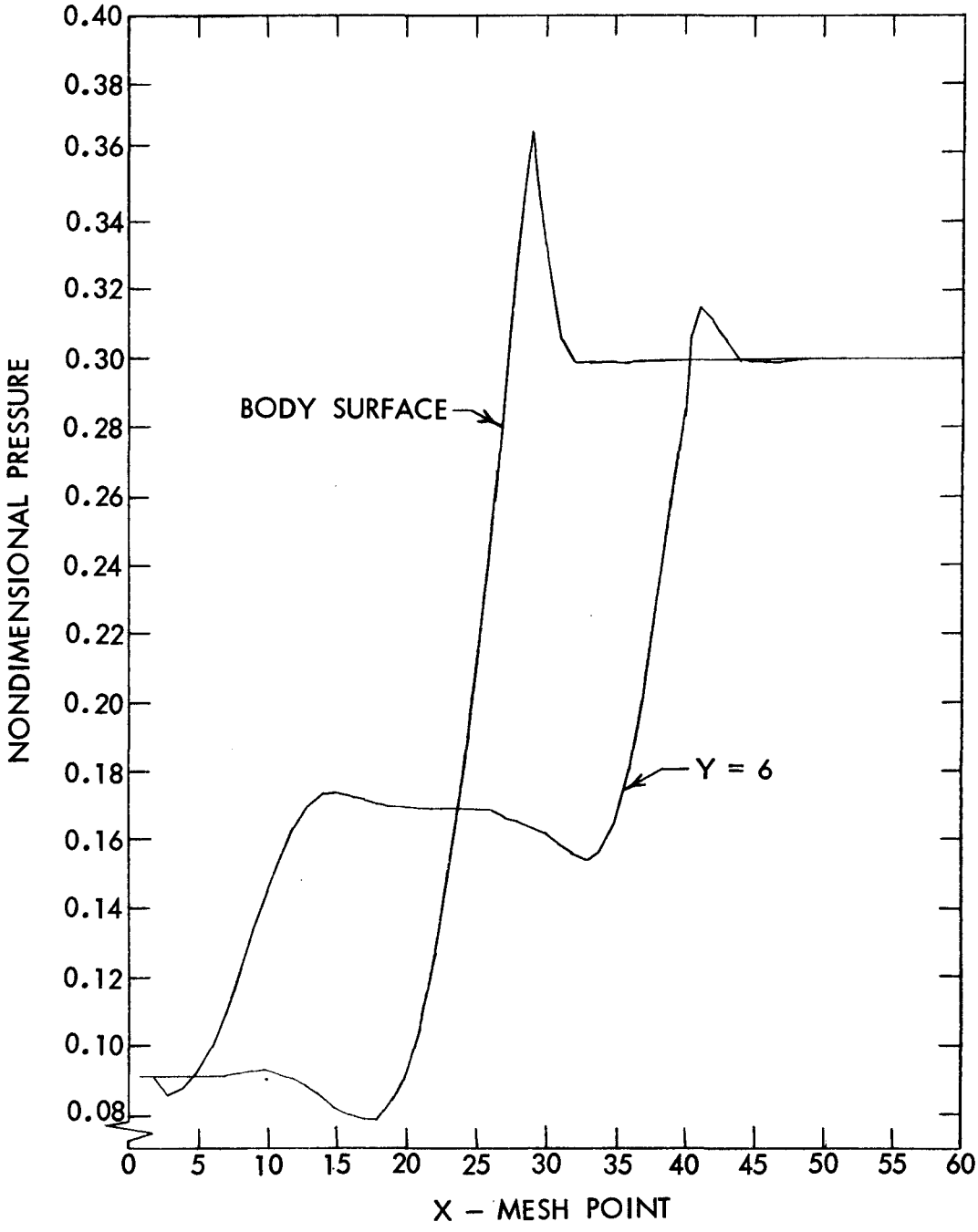

Fig. 17. Shock reflection, Rusanov method, $M_\infty = 2$, $\theta_s = 41^\circ$, $\Delta x/\Delta y = 0.375$, $\delta = 2$.

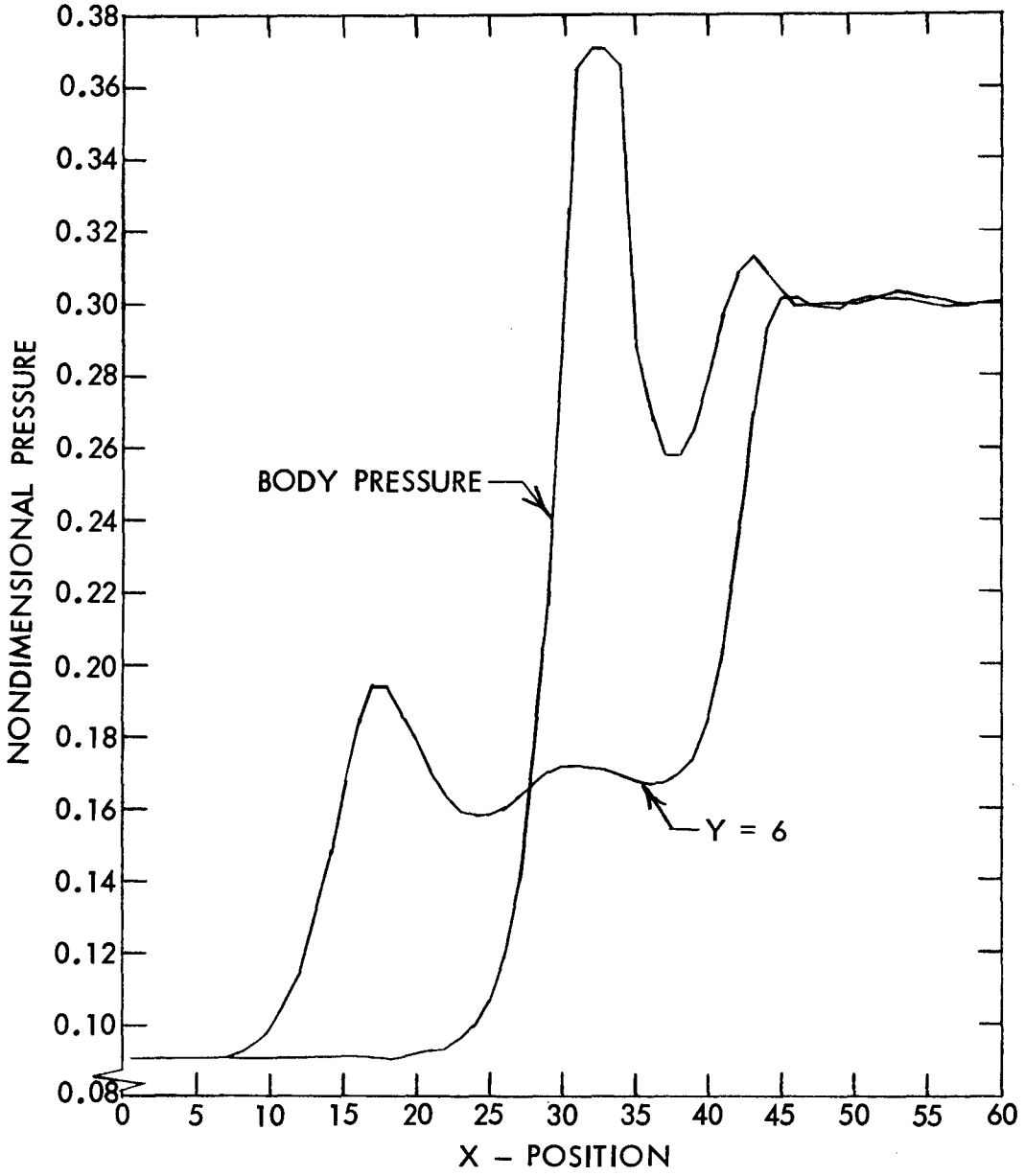

Fig. 18. Shock reflection, MacCormack method, M = 2, $\theta_s = 41^o$, $\Delta x/\Delta y = 0.375$.

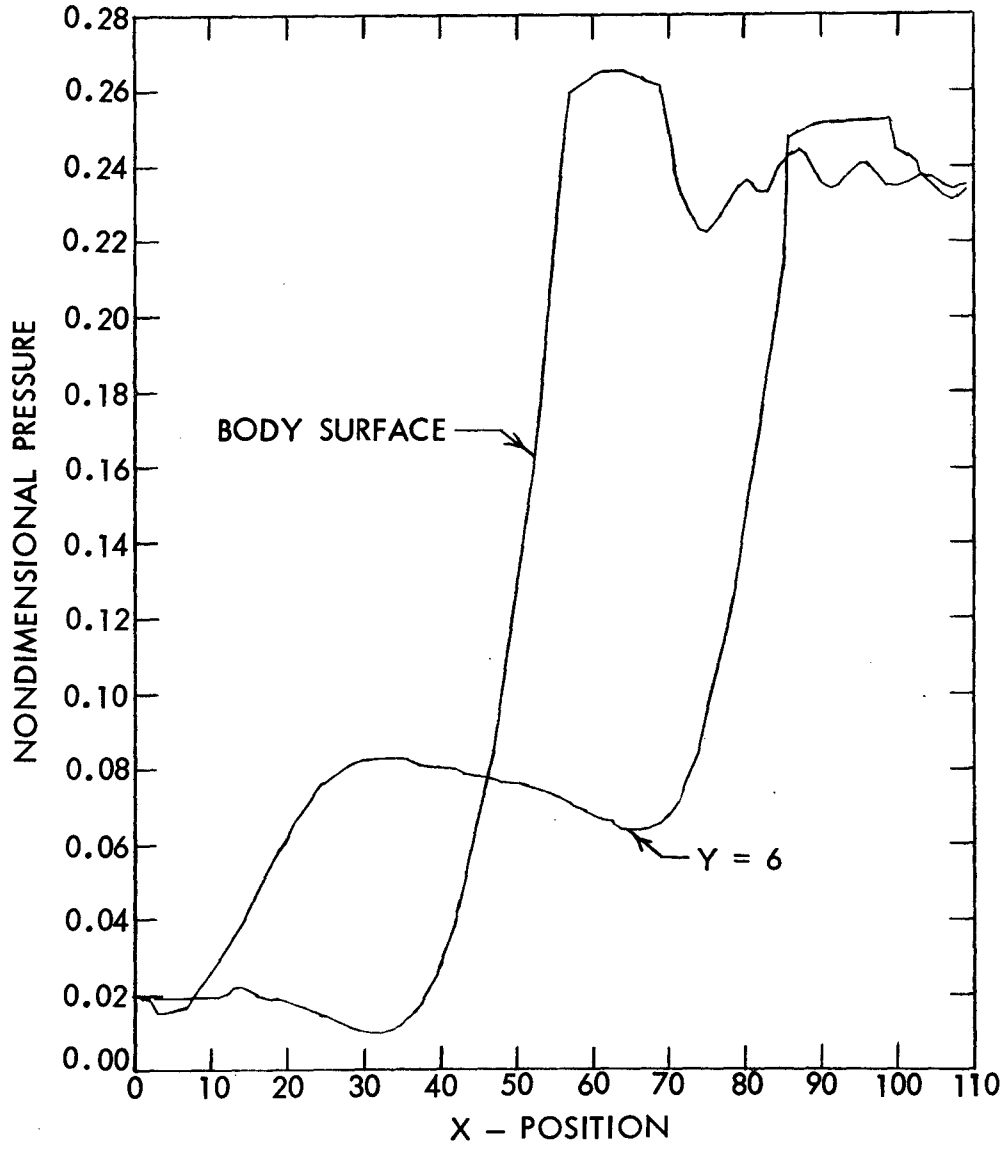

Fig. 19. Shock reflection, Rusanov method, M = 3, $\Delta x/\Delta y = 0.2$, $\theta_s = 39^o$, $\delta = 2.0$.

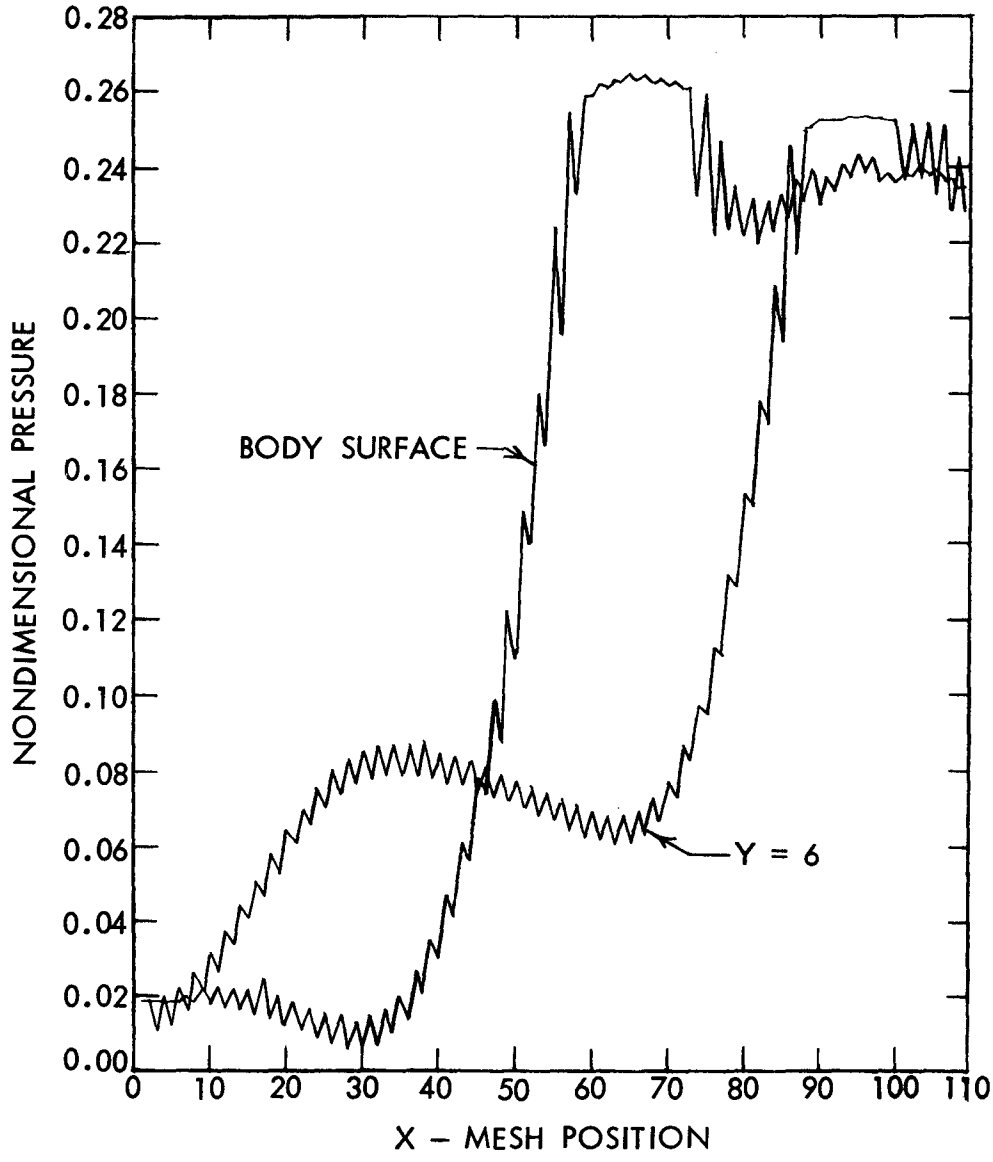

Fig. 20. Shock reflection, Rusanov method, M = 3, θ_s = 39°, $\Delta x/\Delta y$ = 0.2, δ = 3.

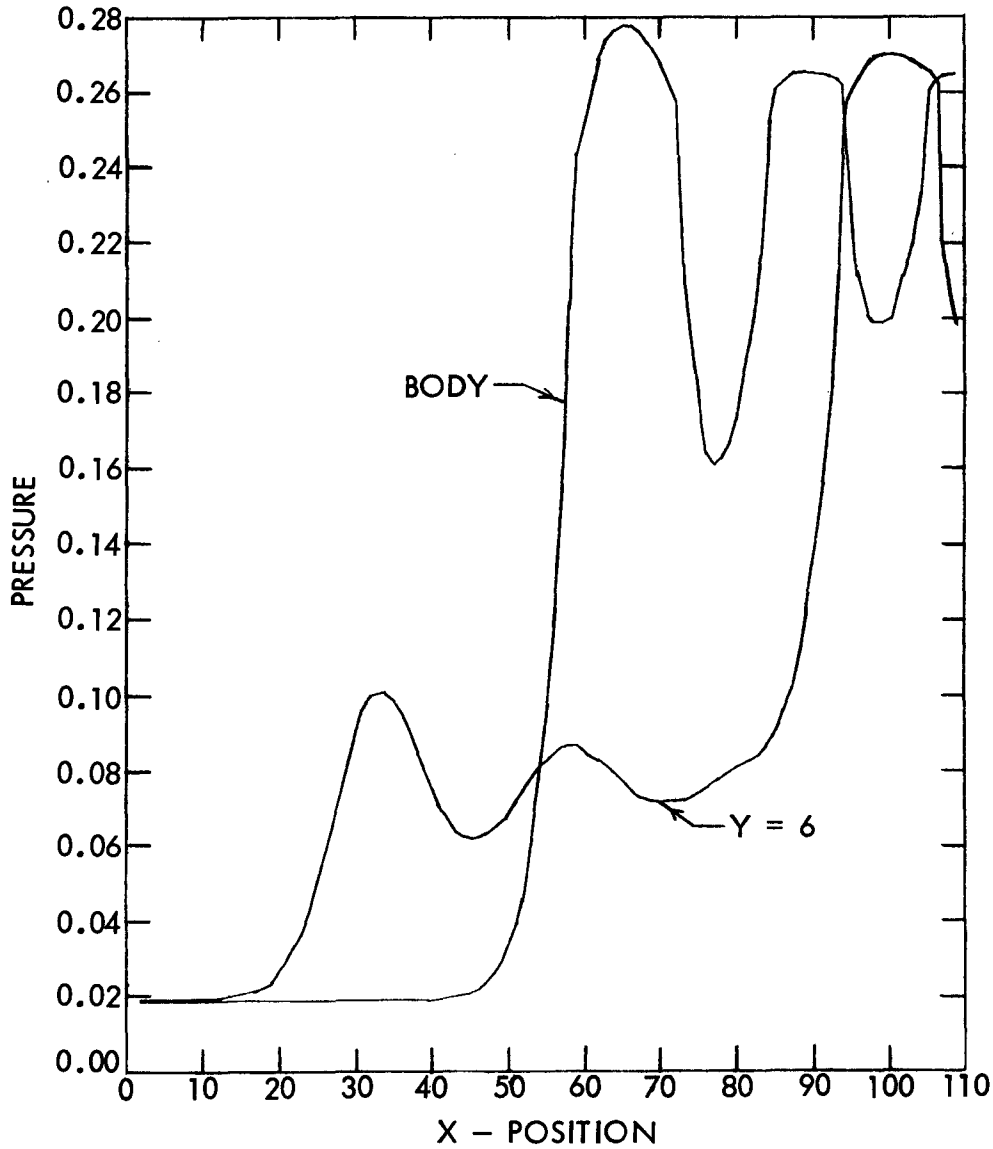

Fig. 21. Shock reflection, MacCormack method, $\Delta x/\Delta y = 0.2$, $M_\infty = 3.0$, $\theta_s = 39^o$.

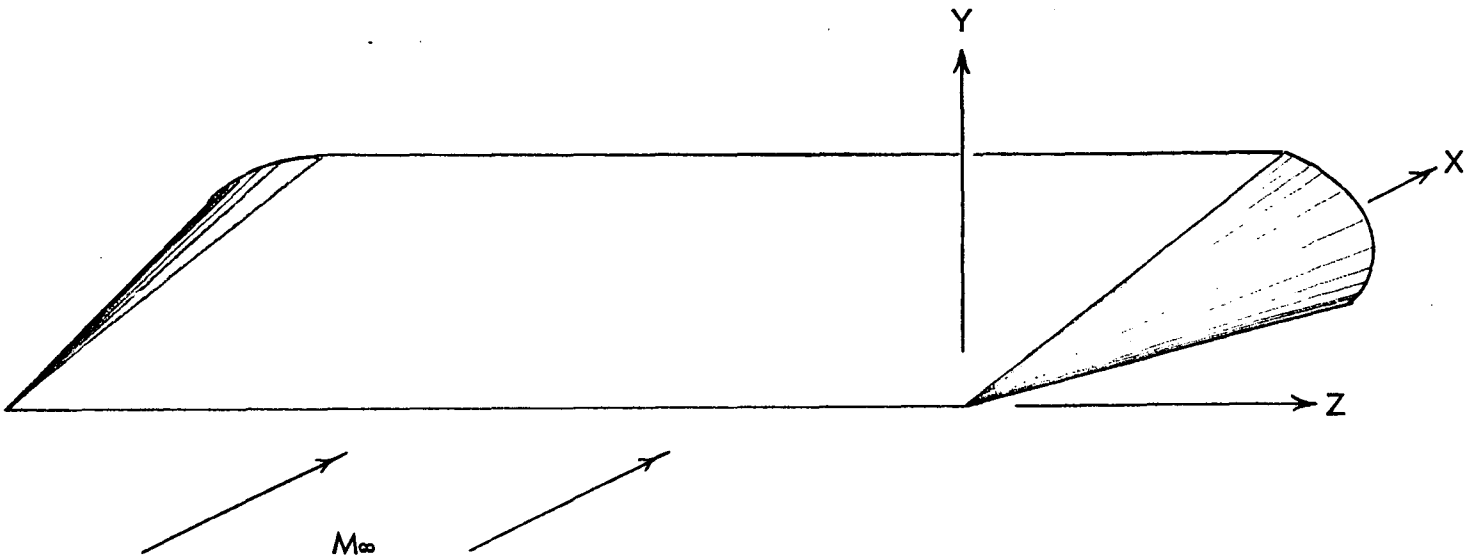

Fig. 22. Assumed leading edge geometry.

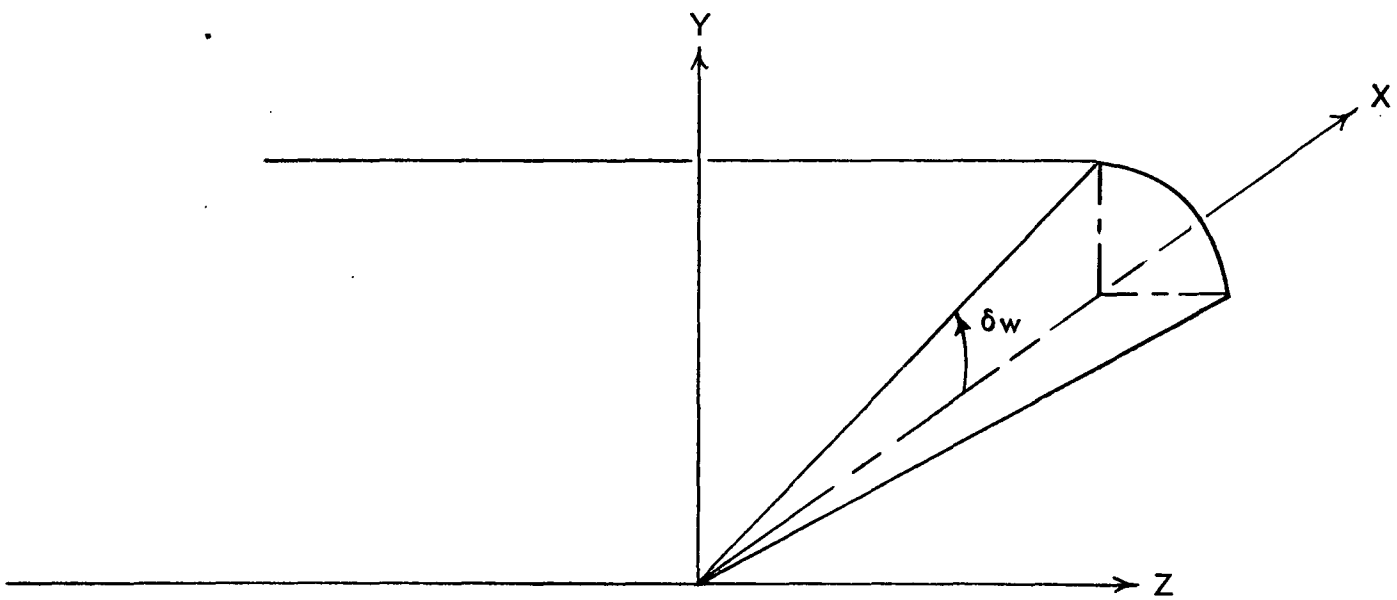

Fig. 23. Cone tip geometry.

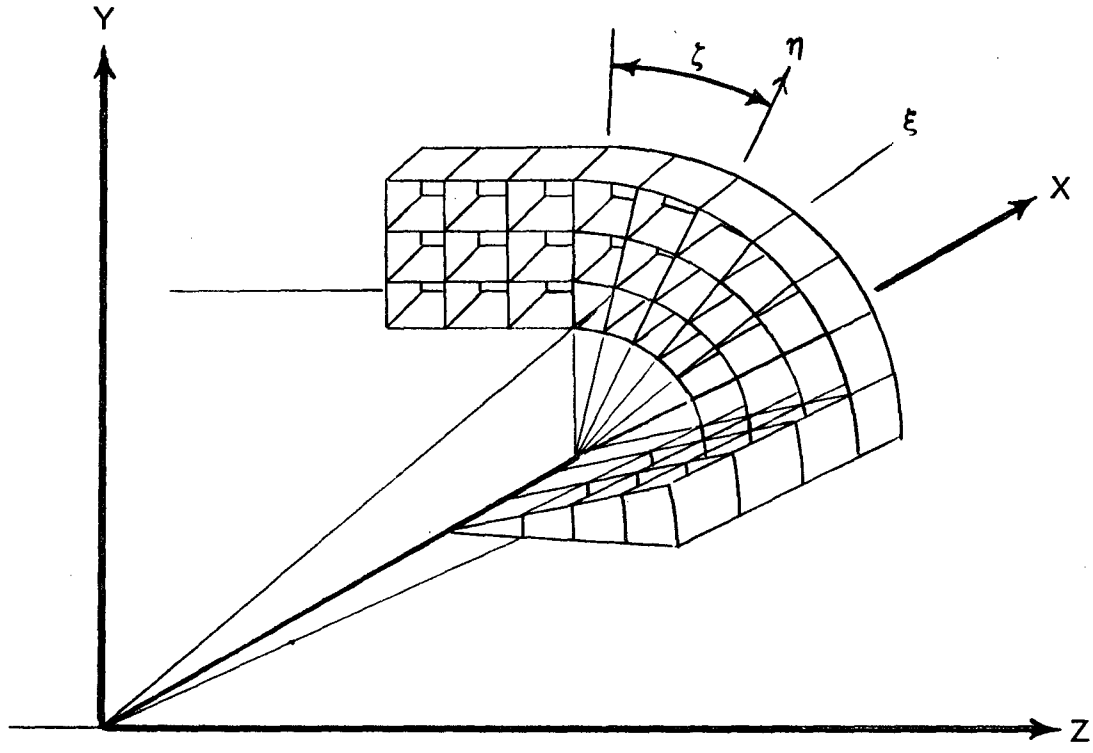

Fig. 24. Body coordinate system.

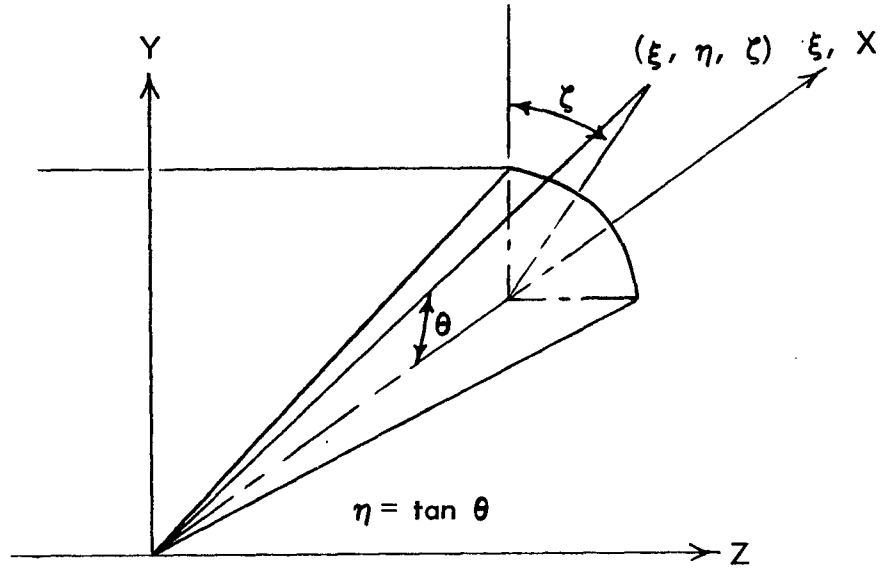

Fig. 25. Cone tip coordinate system.

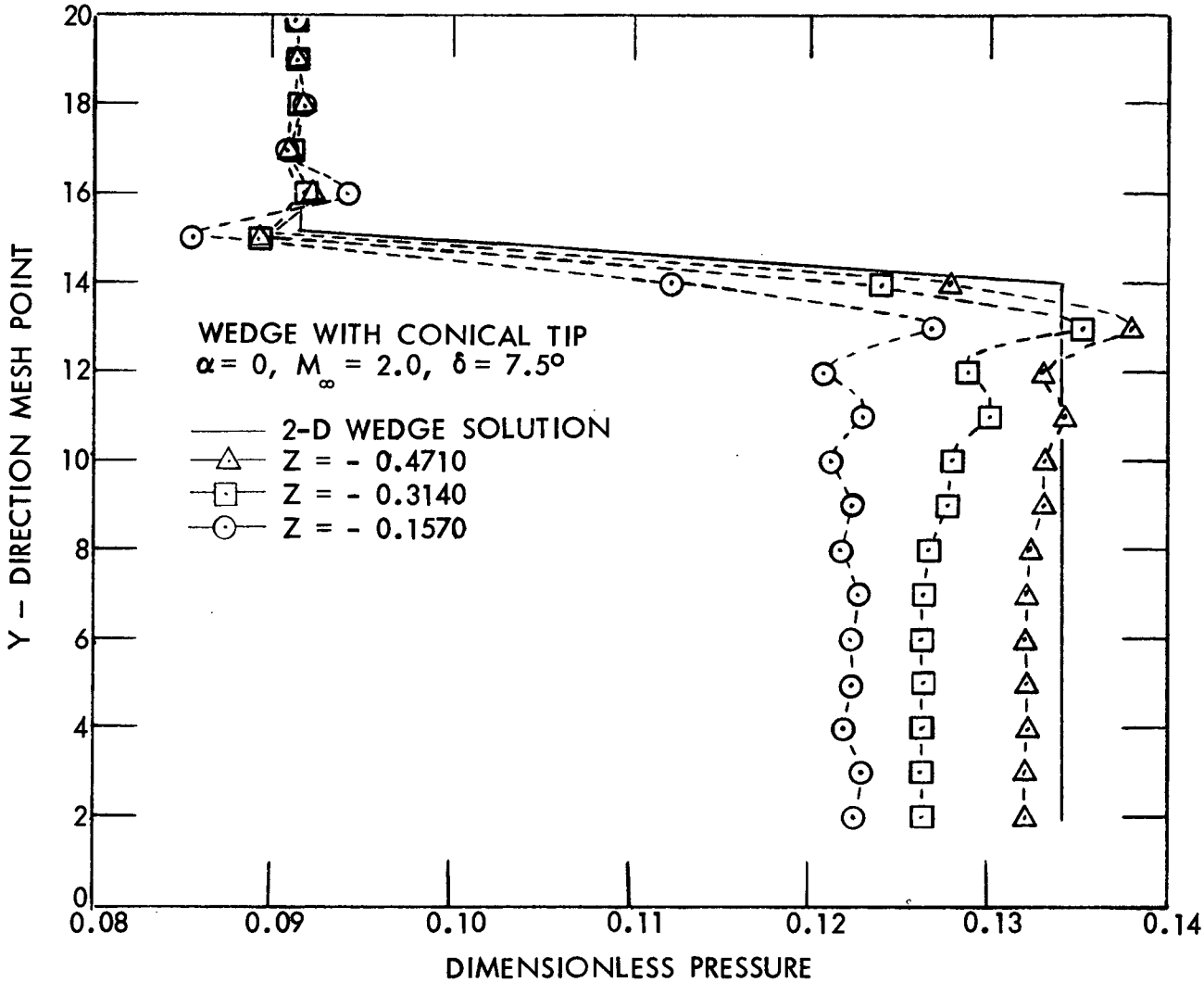

Fig. 26. Normal pressure distributions at various stations along the wedge portion of the wedge-cone combination.

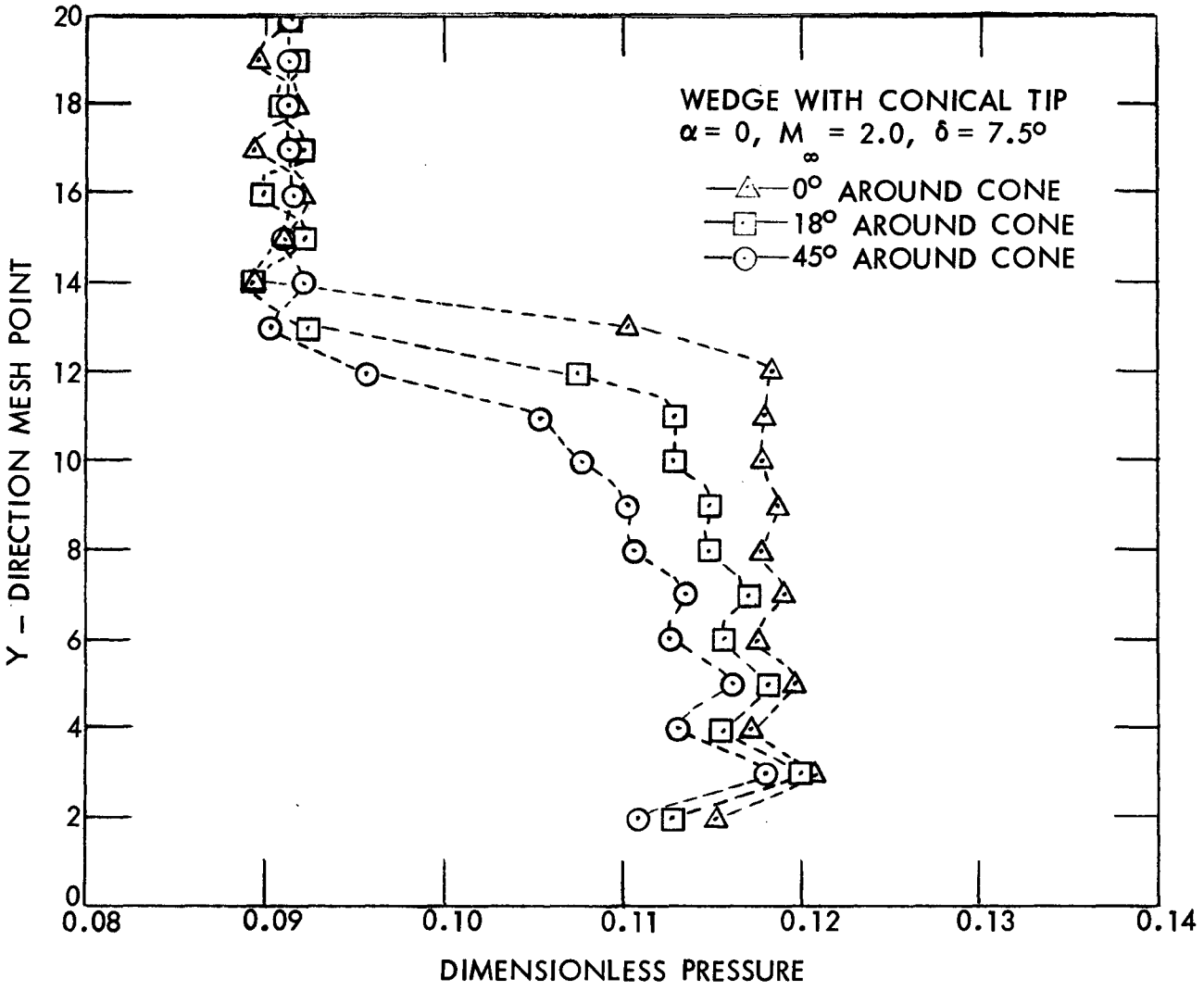

Fig. 27. Normal pressure distributions at various stations along the cone portion of the wedge-cone combination.

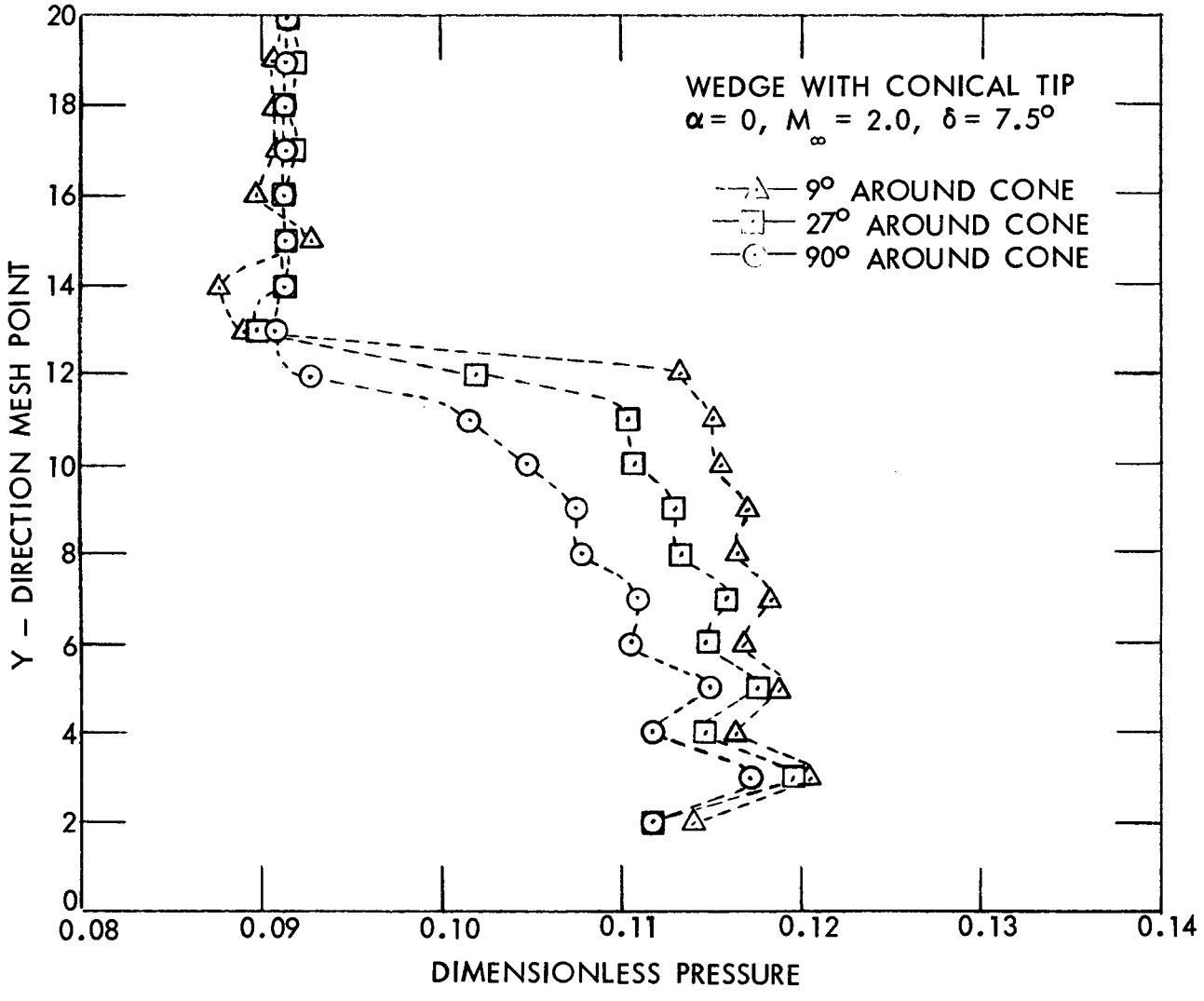

Fig. 28. Normal pressure distributions at various stations along the cone portion of the wedge-cone combination.

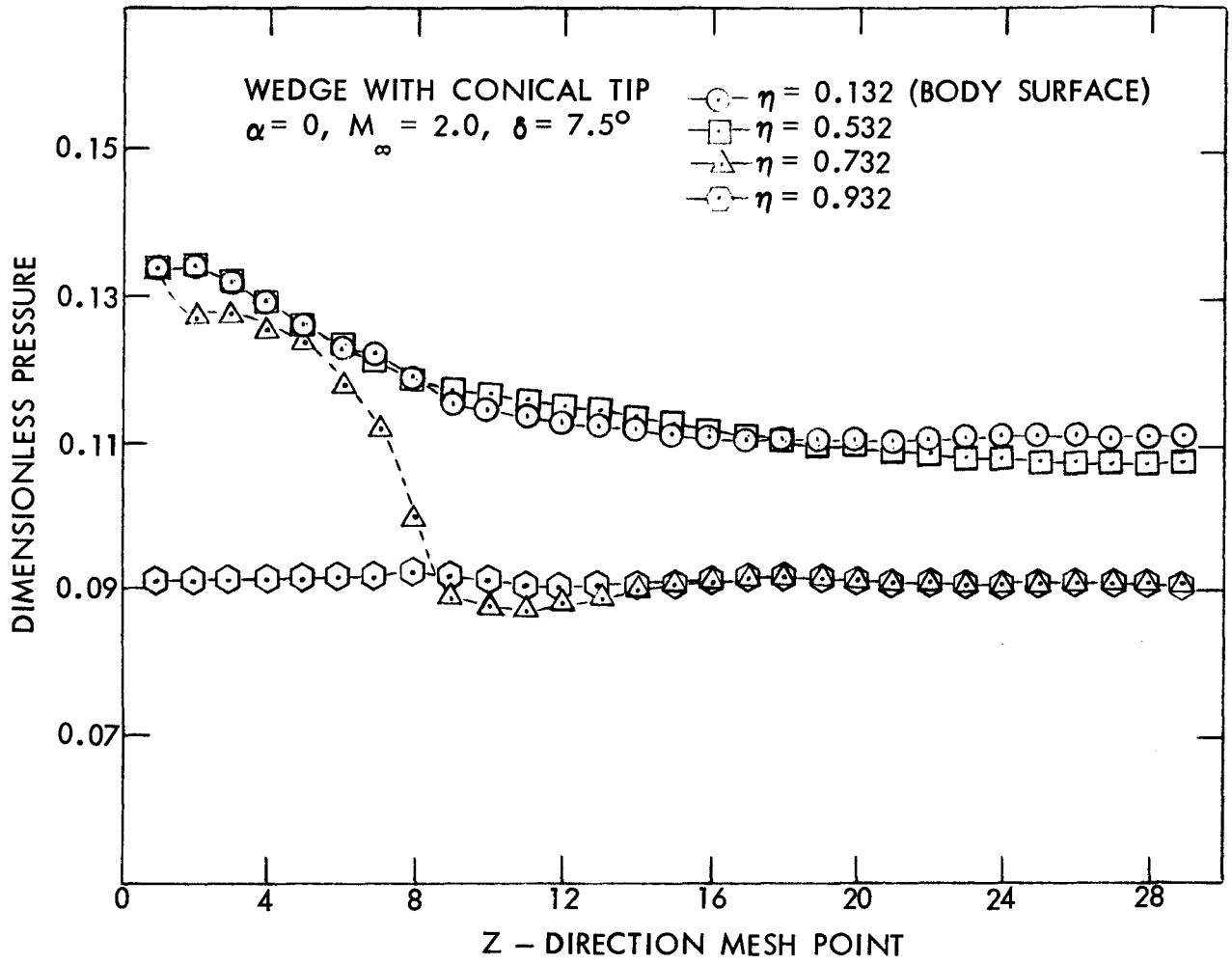

Fig. 29. Lateral pressure distributions along various constant η surfaces for the wedge-cone combination.

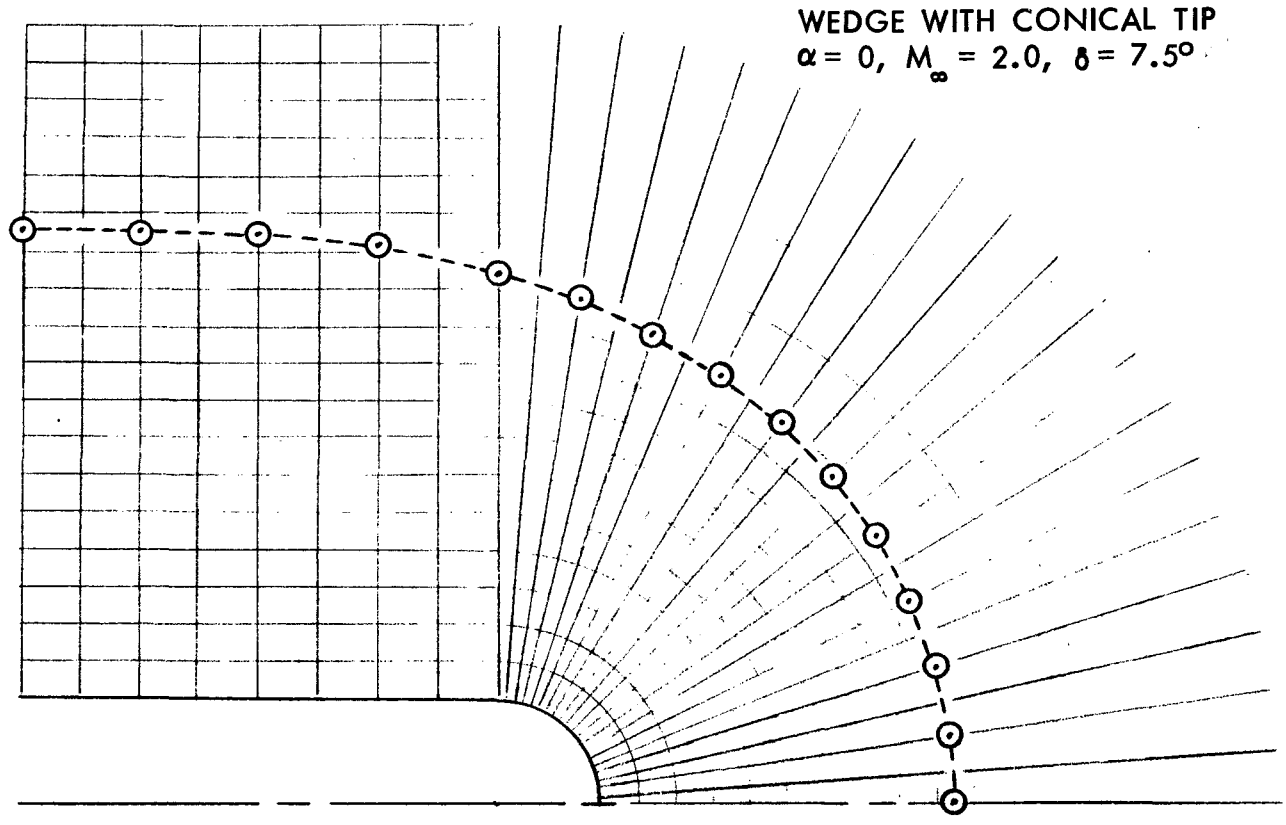

Fig. 30. Shock shape about the wedge-cone tip in the x = 1.0 plane.

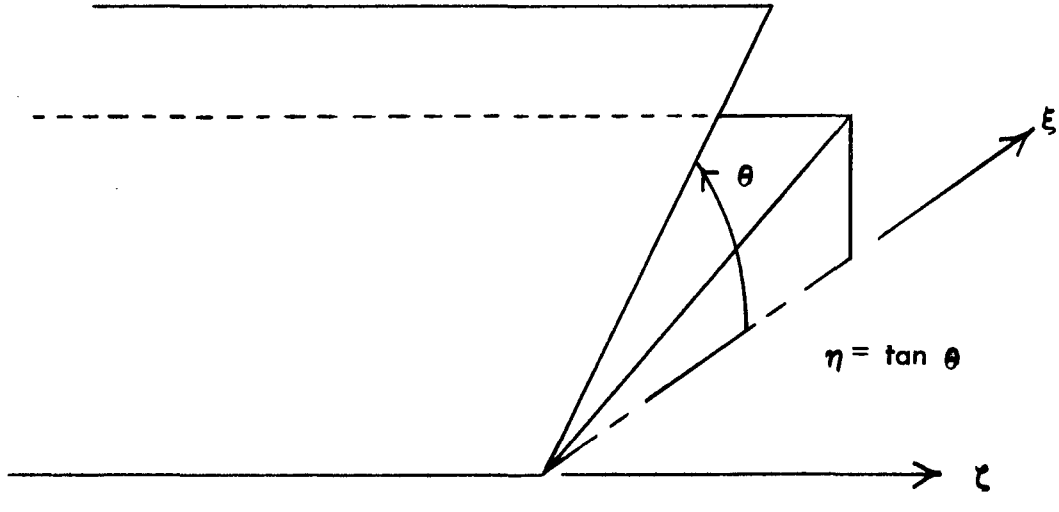

Fig. 31. Square tip coordinate system.

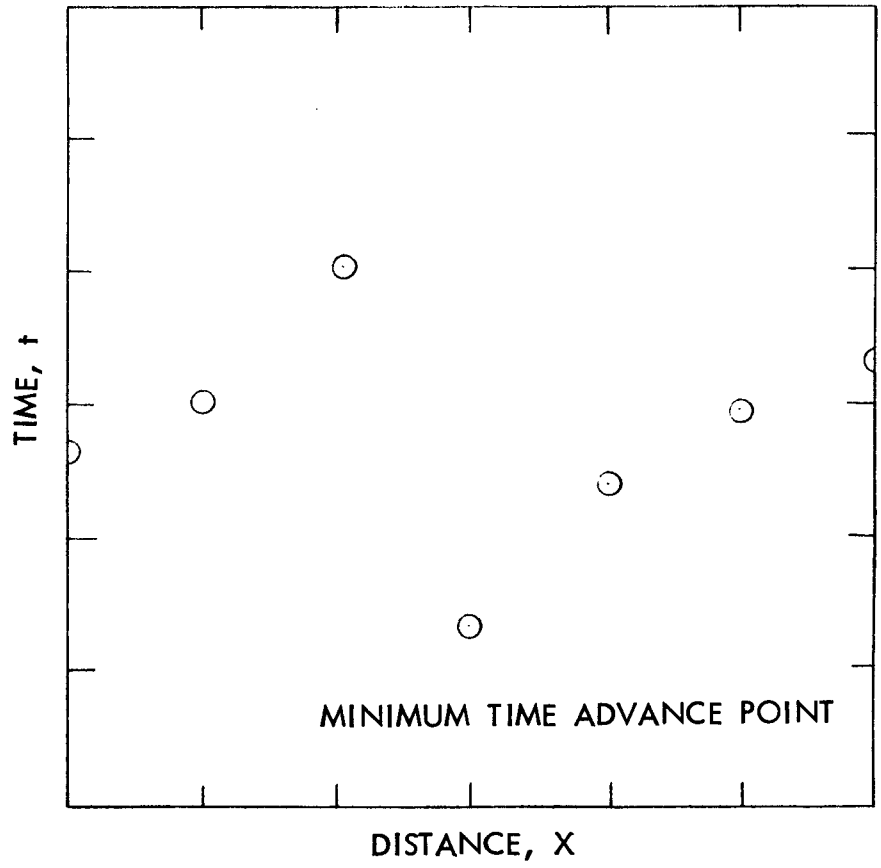

Fig. 32. Optimum difference single step time advance.

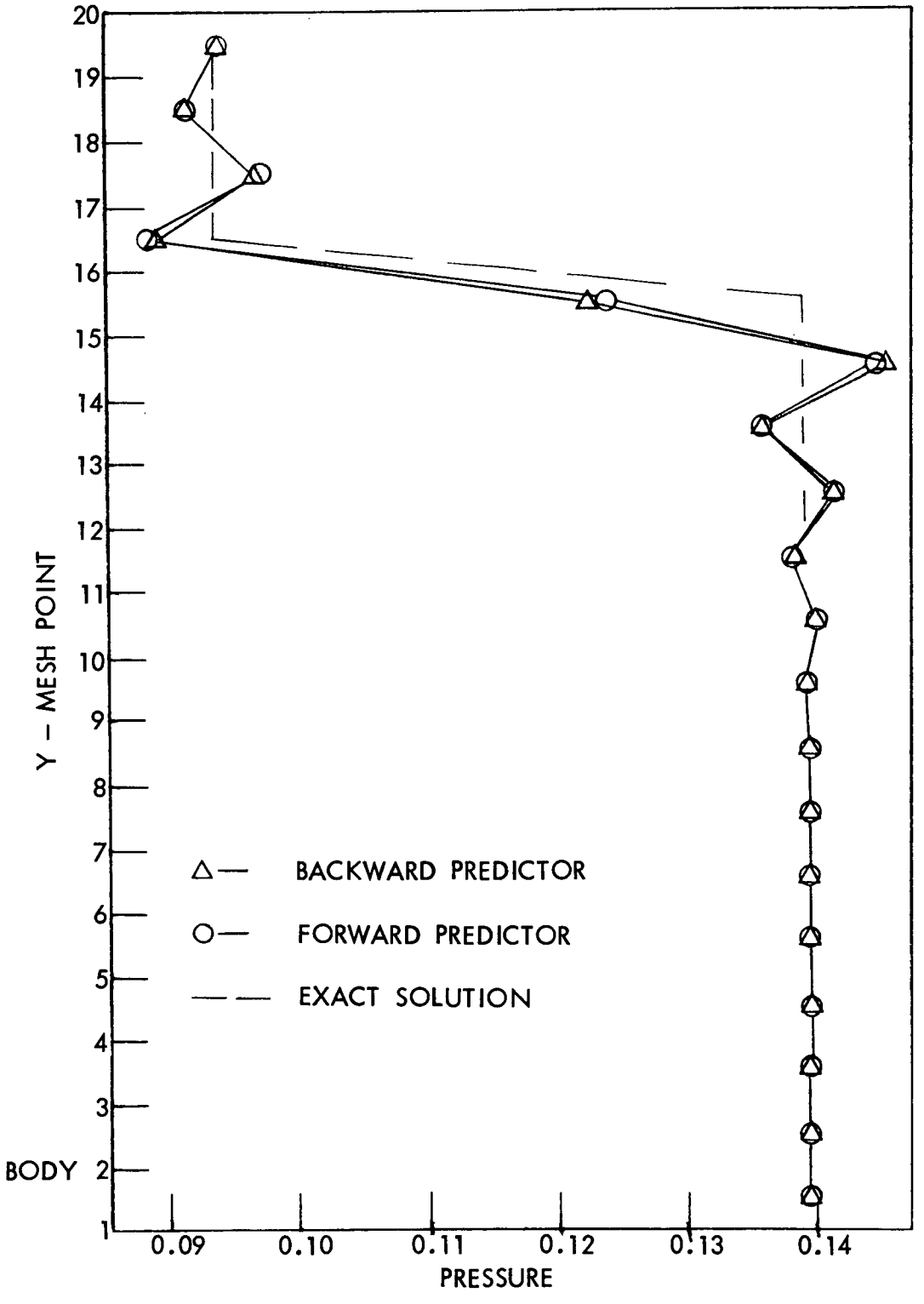

Fig. 33. Optimum wedge solutions, M_∞ = 2.0, local Courant number = 1.0.